Preprint of paper
P. Ripka , M. Mirzaei, J.Blazek: Magnetic position sensors, Measurement Science and Technology 33 (2022) Number 2, 022002,
https://doi.org/10.1088/1361-6501/ac32eb

Magnetic position sensors

Pavel Ripka, Mehran Mirzaei
Czech Technical University in Prague

Josef Blažek
Technical University and EDIS in Košice, Slovak Republic

Abstract

Magnetic position sensors are popular in industrial and automotive applications since they are robust, resistant to dust and oil and they can be cheap. This was traditionally accompanied by low accuracy. However, new precise magnetic position sensors were developed, which can

achieve 0.015 % error and 10 nm resolution. The maximum achievable range is about 20 m. DC magnetic position sensors are using a permanent magnet as a field source; magnetic field sensor is measuring field from that source, which is a function of distance. As a field sensor, magnetoresistors are often used instead of traditional Hall sensors. Eddy current position sensors work also with non-magnetic conduction targets. Magnetostrictive position sensors are based on the time-of-flight of the elastic wave excited in the magnetostrictive material. These sensors can be several meters long and their applications range from level meters to hydraulics.

Magnetic trackers and long-range position sensors utilize AC field sources, which are detectable from distances up to 20 m. Compared to optical instruments magnetic trackers do not need direct view. Their applications include surgery, mixed reality, and underground and underwater navigation.

.

Keywords

Magnetic sensor, position sensor, position detector, position transducer, proximity switch, magnetic tracker

1. Introduction

Magnetic position sensors are popular for industrial, automotive, aerospace, security, and defense applications [1] [2-4]. They are cheap, precise, reliable, rugged, and durable and they are resistant to dust and dirt [5, 6]. Magnetic field generated by these sensors is perfectly safe [7]These devices are sometimes called position transducers. In this paper we are using the more common term “position sensor” and to avoid ambiguity, we clearly distinguish them from magnetic field sensors.

Magnetic position sensors can measure either linear or rotational position. Their output forms are summarized in Fig. 1: the output may be bistable (proximity switch), linear, encoded, or combined. Encoded output is either digital (absolute position sensors), pulse (incremental sensors) or PWM modulated. Combined output has a rough code scale or incremental scale and fine linear scale [8].

Taxonomy of magnetic position sensors is shown in Fig. 2. The moving core or

external target, whose position is measured, may be a permanent magnet (induction position sensors), soft magnetic material (LVDT, variable reluctance sensors), or any electrically conducting material (eddy-current position sensors). Most of the DC magnetic position sensors use permanent magnets as a field source and usually have only mm or cm range, but the compass utilizes the omnipresent Earth's field. AC inductive position sensors use electromagnetic induction and they may work up to a distance of 20 m.

In this paper we make an overview of existing systems and present novel results from the research laboratories, basing it on [1] (with a kind permission from Artech) and [4]. We will also present industrial applications such as in pneumatic and hydraulic cylinders, for underground drilling, large mining machines, and for detecting ferromagnetic objects.

While the most precise inductive position sensors have a resolution of 10 nm and linearity of 0.2 %, precision requirements on the industrial sensors are less demanding, but they should have a large working distance and large resistance to environmental conditions and interference.

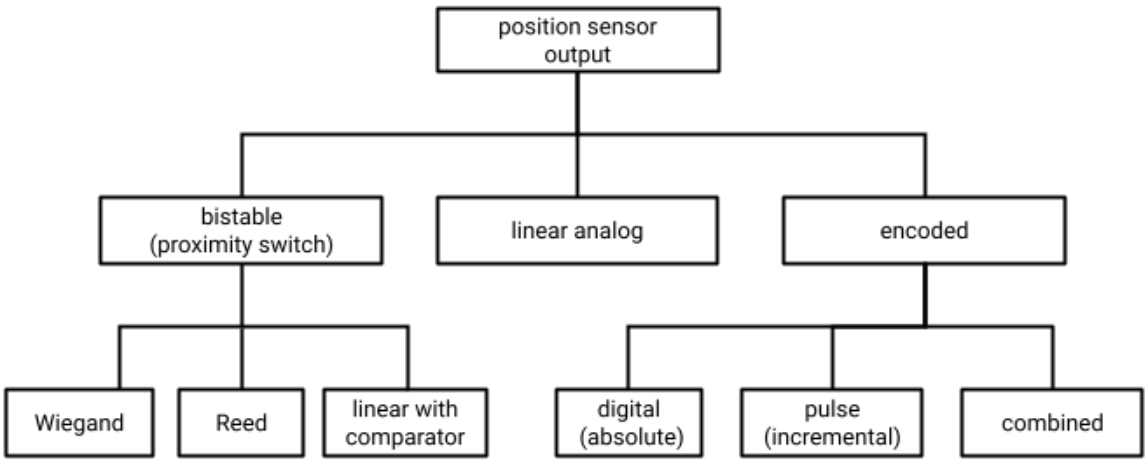

Fig. 1: possible types of sensor output

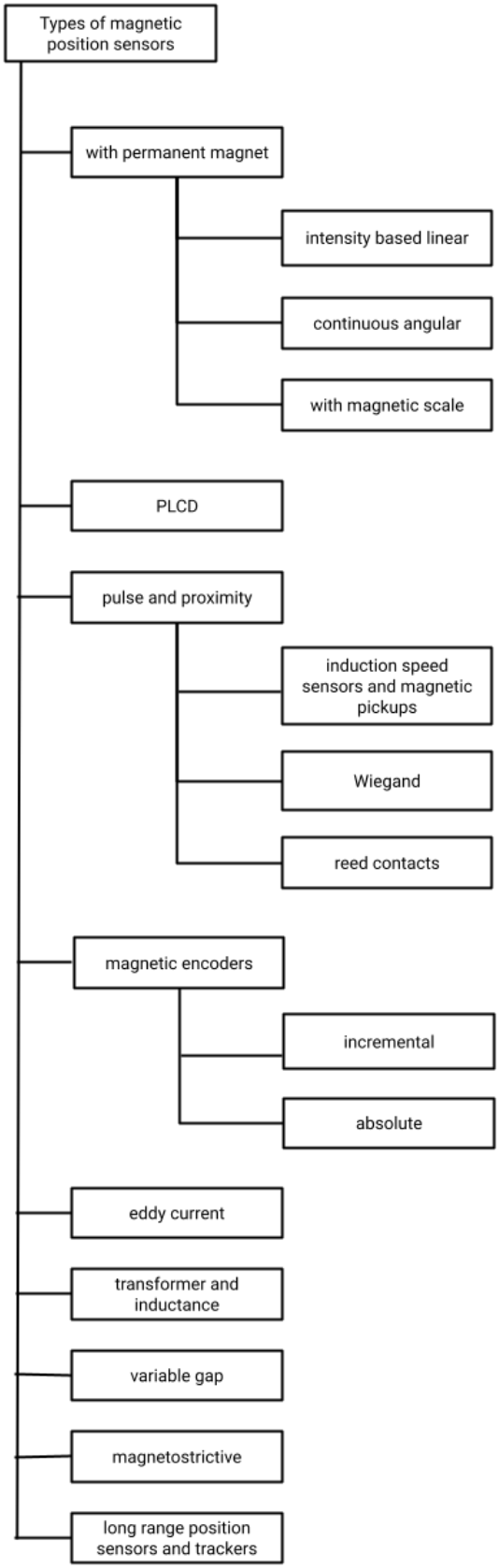

Fig. 2: Taxonomy of magnetic position sensors

2. Position sensors with permanent magnet and magnetic scales

Position sensors of this type consist of a magnetic field sensor, which measures the field of a permanent magnet. This magnet is either connected to the target, or the magnet is attached to the sensor and the ferromagnetic target is moving. Modern designs use more often moving-magnet principle.

The most often used are Hall sensors, and AMR, GMR, and TMR magnetoresistors. Rarely used are semiconductor magnetoresistors and fluxgate sensors. Passive induction coils can detect only field changes. They are used in speed sensors, also called magnetic pickups.

Magnetic scales are made by creating magnetic poles on a tape or a wheel made of semihard material similar to those used in magnetic storage systems.

2.1 Magnetic field sensors for position sensing

Traditional Hall sensors measure in the direction perpendicular to the device plane. They suffer from temperature dependent offset. Modern Hall microsystems suppress offset by using current spinning technique. These devices can measure magnetic field in two or three perpendicular directions thanks to integrated ferromagnetic field guides.

Anisotropic magnetoresistors (AMR) have lower noise and better temperature stability than Hall sensors, but they have limited range to typically 1 mT (100 μT for precise AMR for compass). For precise application they need flipping, which increases the power consumption.

GMR sensors give 360° response for angular sensing and TMR magnetoresistors have very small power consumption and can be made very small.

Fluxgate sensors are the most precise solid state room temperature vectorial magnetic field sensors, but in the traditional form they are expensive and power consuming. Integrated fluxgate appeared recently.

More on magnetic field sensors can be found in [1].

2.2 Intensity based linear distance and position sensors

A small magnet far from the sensor behaves like a dipole so that $B \sim 1/x^3$. This steep dependence causes big errors for larger distances. The range (stroke) can be extended by using a linear array of sensors that may detect zero crossings of the field (Figure 3). An overview of sensors of this type can be found in [3]. This type of sensor may have a resolution of 0.01mm and may work for velocities up to 10 m/s. The achievable uncertainty is well below 1 mm. Linear position module with 3-axial Hall element for gear position sensing in vehicle transmission is described in [9]. The linearity was improved by using a pair of permanent magnets. The achieved error for 3.5 mm airgap is 0.25 mm/30 mm range in the −40 °C to +135 °C temperature range. After the sensor setup calibration, the correction parameters are stored into the sensor electrically erasable programmable read-only memory (EEPROM).

The strategy for determining a magnet position in a 2-D space using 1-D magnetoresistors is described in [10]. Artificial neural network fitting has shown a 5 % error and regression forest fitting methods had a 2.5 % error in the 3x3 mm active area.

Another approach is to use a larger number of permanent magnets [11]. Using three Infineon 3-D Hall sensor TLV493 with resolutions of 100 μT and $Nd_2Fe_{14}B$ magnet array with 20 mm pitch results in 1 mm uncorrected position error even for 4 mm airgap. A combination of permanent magnets and Hall sensors is used in rehabilitation devices and robotics to measure the position of hand and fingers, gesture recognition, and knee angle [12].

If the magnet and sensor are located in a ferromagnetic environment, significant error is caused by the material hysteresis. If the motion is repetitive such as in hydraulic cylinders that have ferromagnetic body or elevator position to the rails, partial correction of hysteresis can be made by Kalman filter using a model of magnetic material. RMS

position error of 0.3 cm was achieved for a wall thickness of 12 cm [13]. Using multiple sensors can help to extract the signal from interference and disturbances [14].

One of the limiting factors of precision of these position sensors is the temperature dependence of the properties of the permanent magnet. Alnico magnets have the best temperature stability, but their coercivity is quite small. Permanent magnets from the SmCo group have very good magnetic properties, but their disadvantage is a high price. Currently the most popular are NdFeB magnets, either sintered or molded. Bonded NdFeB magnets are manufactured mainly in the isotropic version so that they can be magnetized in all directions and multipole magnetization is possible [15]. Specifications of typical industrial sensors of this type are shown in Table 1.

Intensity-based magnetic position sensors need a source of a magnetic field either in form of a permanent magnet or coil. It is not a good idea to rely on natural sources, such as remanence of steel or iron parts, or Earth's field. Such wrong concepts used in [16] should fail as the remanence of magnetically soft materials depends on their temperature and magnetic history. Subjecting the steel part to a strong magnetic field would destroy the sensor calibration. If one decides to use the Earth's field in position meter, the device reading depends on its orientation which is hardly acceptable.

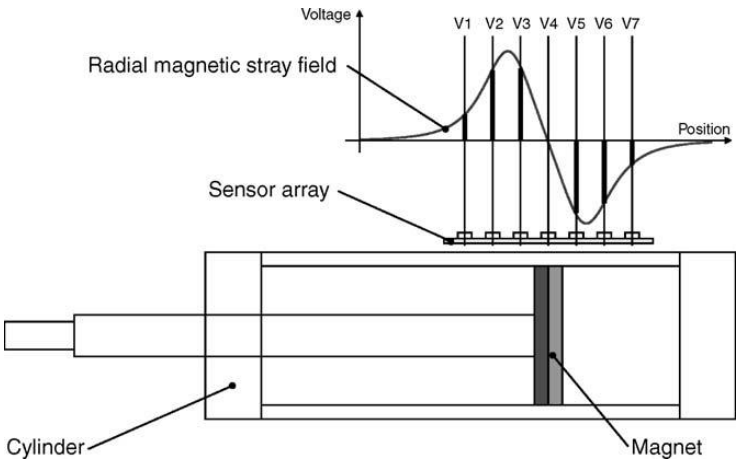

Figure 3. A linear sensor array for position sensing of a piston in a pneumatic cylinder. From [3] with permission from Elsevier

type	Min range (mm)	Max range (mm)	Resolution (μm)	Field range	Linearity
SICK MPA	100	1 007	0.03 % FS (max.≥ 60 μm)	2 mT .. 15 mT	0.5 mm
Festo SDAT-MHS	80	160	50		±0.25 mm
MHL 1400 by Active Sensors	5	300	0.025% FS	Internal magnet	0.4 % FS
Honeywell SPS	35	225	3.5 μm	Airgap 8.5 mm	0.4 % FS

Table 1 Specification of the magnetic linear distance sensors with moving permanent magnet. FS is a full scale of the sensor.

2.2 Continuous angular sensors *(end of the shaft)*

A permanent magnet can be also attached to the end of the shaft. In this case, GMR spin valves and also TMR sensors are ideal for angular sensing in saturated mode (Fig. 4) [17]. The free layer is rotated by the magnet. Once the layer is saturated, the output depends only on the angular position and not on the distance between the sensor and the magnet. Two perpendicular sensors are used to achieve a 360° range. Properties of typical industrial types of end of shaft sensors are shown in Table 2.

Integrated angular sensor based on a circular array of vertical Hall sensor is described in [18]. The sensor was developed for space applications; it has a maximum error of 0.5 deg which was not degraded after a radiation dose of 50 krad (Si).

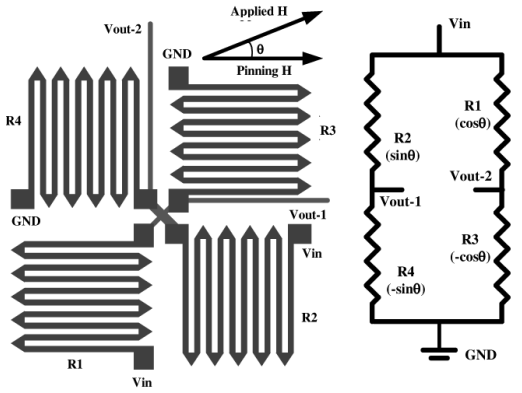

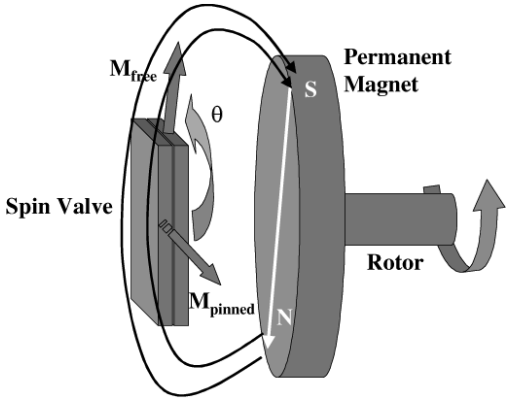

c)

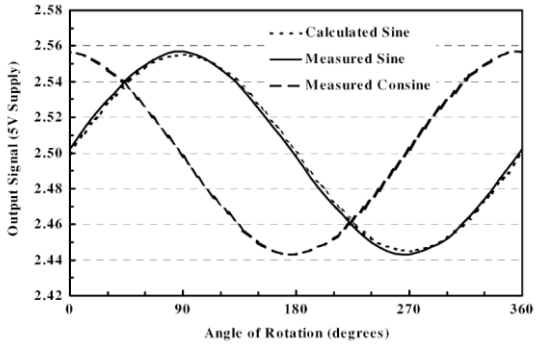

d)

Figure 4. An angular rotation end-of-shaft sensor with GMR: a) layout of the sensor, b) circuit diagram, c) configuration of the permanent magnet and sensor, d) sensor outputs © 2005 IEEE Reprinted, with permission, from [17].

type	technology	Required field (mT)	Resolution (deg)	Max. Speed (rpm)	Linearity error (deg)	Error in -40 to 150º C range (deg)

AS5048 by PMT	Hall	30..90	0.06	456	0.8	1.2
KMA 36 by TE connectivity	AMR	18 .. 75	0.045		0.3 < 1	
AAS by Allegro	Hall	30	0.22	15 000	0.4< 1	0.7<1.3
MLX90380 by Melexis	Hall	10..70	0.25 (est.)	25 000	0.5	1

Table 2 Specification of the rotational end of shaft magnetic position sensors

2.3 PLCD (Permanent magnetic Linear Contactless Displacement sensor) [1]

The Permanent magnetic Linear Contactless Displacement sensor (PLCD) is shown in Fig. 5. The sensor consists of a long magnetic strip core with the homogenous secondary winding. The primary winding has two sections connected antiserially, which are supplied with ~4 kHz sinewave. A permanent magnet in the core vicinity creates a saturated region that magnetically divides the core into two halves whose lengths determine the signal induced into the secondary winding [19]. The induced voltage is processed by the phase-sensitive detector to obtain the linear output. The typical resolution is 0.2 %, linearity 1% FS, which is between 20 mm and 150 cm. Compact PLCD sensors can be fabricated by microtechnology or PCB technology using a strip of amorphous magnetic materials as a core. The winding is made using copper layers interconnected by vias or by electrodeposition [20].

The main advantage of PLCD is that the device is immune to changes in the air gap between the magnet and core. The applications include automotive and hydraulic cylinders.

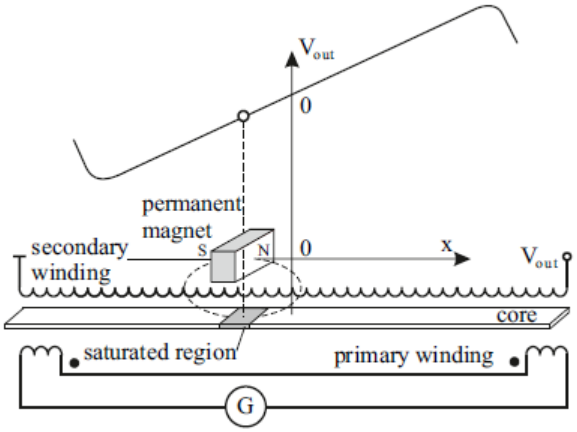

Fig. 5: PLCD sensor

2.4. Pulse-output sensors and proximity detectors

These sensors have bi-stable (digital) output. They may be either activated by a moving magnet, or biased by a fixed magnet, and activated by a magnetically soft target. A typical example of a naturally bipolar sensing element is a reed contact. Any magnetic sensor with analog output followed by a comparator or Schmidt trigger can be used as a position detector. The most popular are Hall sensors, AMR, and recently also GMR magnetoresistors and also some semiconductor magnetoresistors.

2.4.1 Induction speed sensors and magnetic pickups

Induction sensors with a moving magnet are also called **"speed sensors"**. The target is a permanent magnet and the sensing element is an induction coil, either an air coil or more often coil with a ferromagnetic core. These sensors are based on the induction effect, they consume no energy, but the output depends on the target speed. Thus, these sensors fail at low

speeds.

Variable reluctance sensors with fixed permanent magnets are also called **"magnetic pickups"**. The sensing element is again induction coil, the DC field is also generated by a permanent magnet, which is fixed and the coil flux change is produced by changing the position of the soft magnetic target. The applications include gear tooth sensing in shaft speed measurements and antilock brake systems (ABS); due to low sensitivity at low speeds they are not suitable for car ignition timing systems.

2.4.2 Wiegand sensors

Wiegand patented in 1981 a revolutionary sensor, which generated a high voltage pulse when the magnetic field reached some threshold value; the shape of the voltage pulse is highly independent of the rate of the field change and the device is passive, having just two terminals [21]. Wiegand made his sensors of 0.3 mm wire from Vicalloy (Co52Fe38V11) which was twisted to cause plastic deformation resulting in higher coercivity in the outer shell and elastic stress in the central part. The central part forms a single domain. The pulse is caused by one large Barkhausen jump when this single domain reverses its magnetization. The pulse width is determined by eddy current damping [22, 23]. 30 mm long wire with 1000-turn coil may generate 7 V pulses. The main disadvantage of the Wiegand configuration is that the outer shell cannot be made really magnetically hard, so it can be unintentionally remagnetized by an external field higher than 25 mT. Therefore, the main application field of Wiegand wires is not magnetic sensing, but marking and security application. Wiegand wires have been also used for energy harvesting and energy transmission [24, 25]. Similar properties have some amorphous glass-covered microwires

2.4.3 Reed contacts [1]

Reed contacts are very cheap and totally passive devices. They consist of two magnetic strips of soft or semi-hard magnetic material sealed in a glass pipe filled with inert gas. Reed contacts have been manufactured also in MEMS technology [26]. Normally open contacts are connected at a certain field by an attractive magnetic force between the free ends. Other contact types are normally closed. The reed contacts have hysteresis and their switching zones have a complicated shape. However, they are still very popular because of their simplicity.

Fig. 6 shows that if the magnet is perpendicular to the contact and moves along with it, there may be two "switch-on" zones. If the contact and magnet have the same direction and the magnet moves along it, there may be three or one switching zones. This behavior is easy to explain by the shape of the magnet field lines.

High security "balanced" switches use two reed contacts in the vicinity of the magnet; one of them is normally open and the other normally closed. Any movement of the magnet causes the transfer of one of the switches. The normally open contacts are usually crossed by a resistor, which allows monitoring the continuity of the wires.

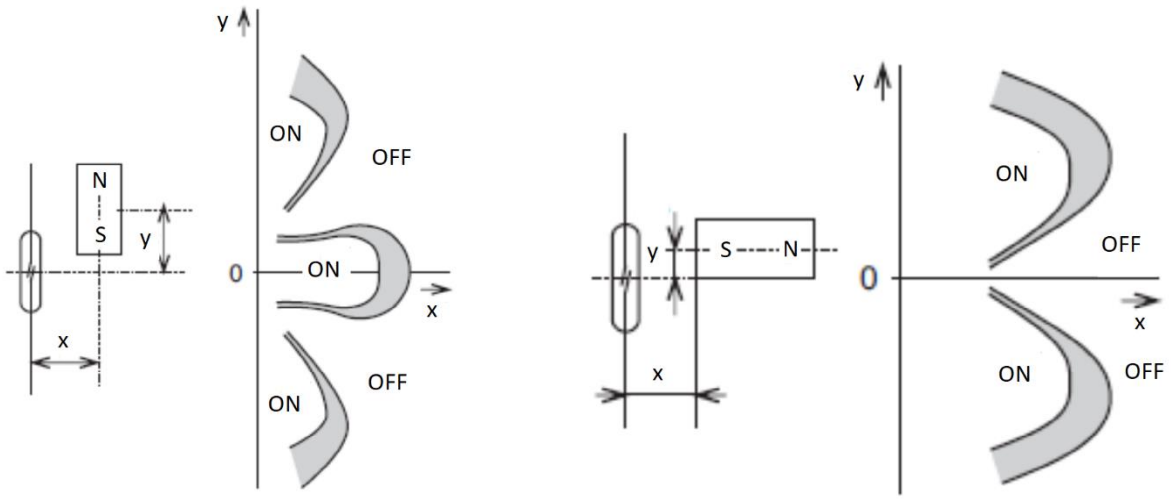

Fig. 6 Switching zones ("ON") of the reed contacts. The sensor state is uncertain in grey

regions due to the sensor hysteresis. From [27]

2.4.4 Eddy current proximity detectors

Eddy current sensors (for any conducting targets) and AC- excited variable gap sensors (only for magnetic targets) are also used for linear or angular gear position sensing. An example of an integrated inductive gear tooth sensor is shown in Fig. 7 [28]. Similar principle is used for high-temperature applications such as speed sensors for gas turbines.

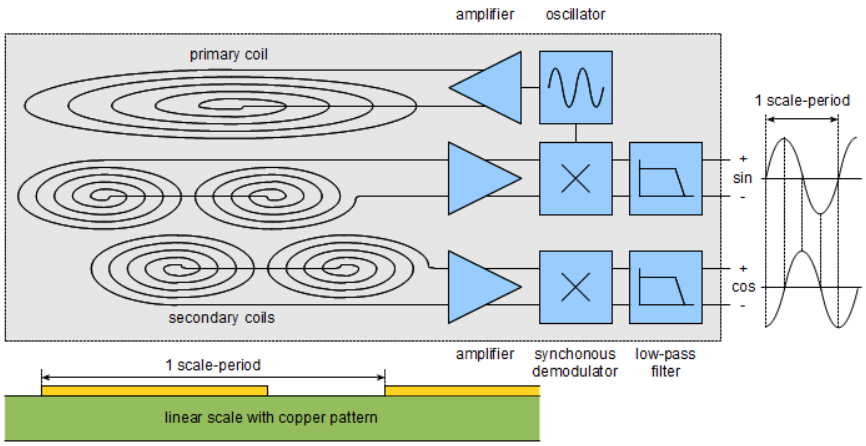

Fig. 7: Block diagram of miniature inductive gear tooth sensor – from [28]© 2008 POSIC SA

2.5. Magnetic encoders (linear and angular)

2.5.1 Incremental encoders

Magnetic encoders can be made both incremental and absolute. Rotational incremental

position sensors with radial permanent magnets are standard devices in the industry. Figure 8 shows the most popular configuration with a multipole ring. The ring is made of magnetically hard material and magnetized by pulse coils to create magnetic marks consisting of domains with the reverse direction of magnetization. The Hall sensor measures the radial component of magnetic field.

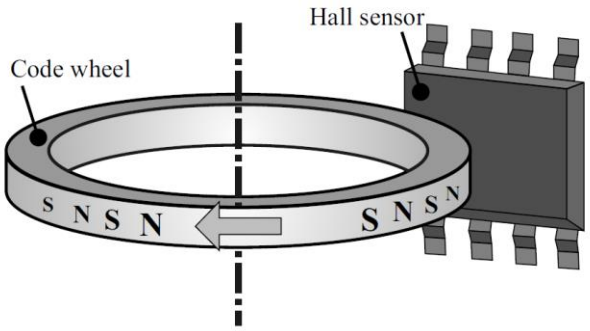

Figure 8. Rotational speed / incremental position sensor with an integrated Hall sensor (Image provided courtesy of Allegro MicroSystems).

The linear incremental encoder works similarly. The typical configuration with AMR sensing bridge is shown in Fig. 9. The pole pitch of the magnetic scale depends on the required separation between the scale and sensors: for a 1 mm pitch the allowed separation is only 0.4 mm; a 5 mm pitch allows 2 mm separation. Both AMR and Hall sensors are being used in this application. The magnetic field measured by two sensors separated by a quarter of the pitch follows a sinewave shape. The fine position can be calculated by using the outputs of these sensors. The achievable resolution is 1/1024 of the scale pitch. For the most precise sensors, correction for reading head displacement and misalignment should be made [29].

The parameters of some sensors on the market are summarized in Table 3.

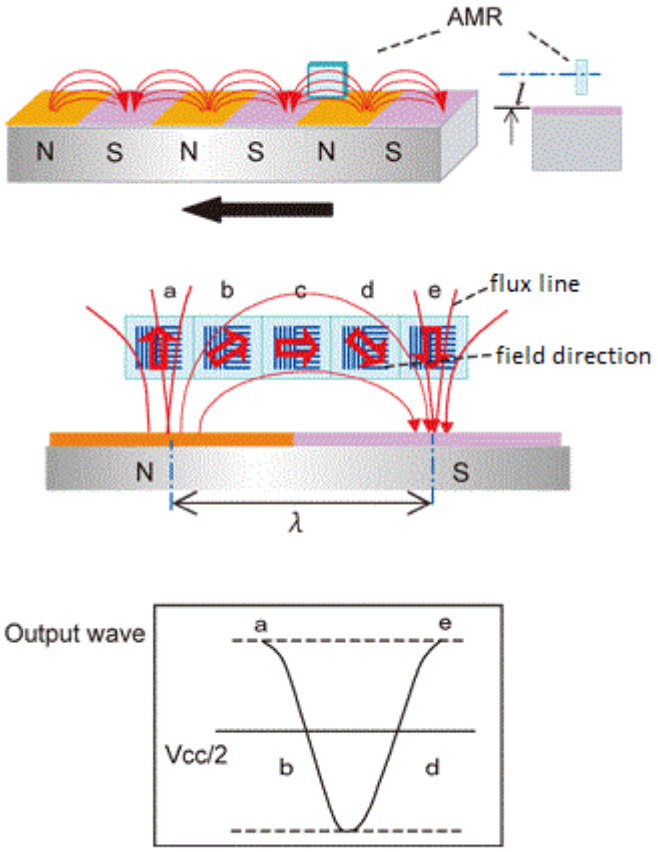

Fig. 9 Linear AMR speed/incremental position sensor – from [30] (courtesy of KOHDEN Co., Ltd).

Some linear incremental encoders utilize a magnetically soft salient ferromagnetic scale, while the field source is a permanent magnet attached to the moving sensors. In the case of a linear motor, the toothed stator can serve as a scale [31]. The sensor is shown in Fig. 10. The field vs. position waveforms are close to sinewaves. One of the design goals is to keep the total harmonic distortion (THD) of these sinewaves low in order to reduce the interpolation error.

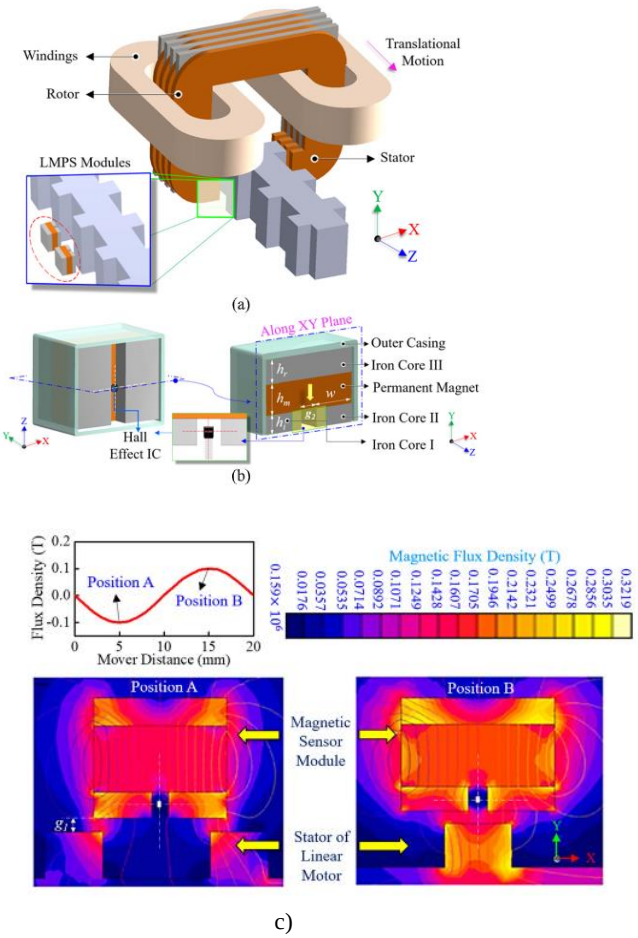

c)

Fig. 10 Linear position sensor based on toothed stator and Hall sensors biased by permanent magnets - from [31]: (a) permanent magnet linear synchronous machine (PMLSM) with the linear magnetic position sensor (LMPS); (b) whole and the sectional view of the LMPS along XY plane highlighting different parameters; (c) 2D flux density distribution plot of the LMPS for two pole pitch movement of the mover

A permanent magnet synchronous linear motor has an inherent magnetic field related to the position. An accurate model of the spatial waveform of this field can reduce the position error. Using an array of 8 Hall sensors and a high-order field model, 5 μm RMS error was achieved [32]. A similar approach has been used for Permanent Magnet Synchronous Motors: the stray field from rotor permanent magnets is sensed by a TMR sensor on the surface of the motor. The achieved velocity error is 0.5 % over the speed range from 50 to 1000 rpm [33].

Type	Pole pair length (mm)	Resolution (μm)	Max. Speed (m/s)	distance / field range	Absolute error (μm)	System error (μm)
NSE 5310 by PMT	2	0.5	0.65	10..40 mT	10	40

KMXP by TE connectivity	1			0.4 mm	10	
	2			0.8 mm	20	
	5			2 mm	50	
Baumer MIL 10	2	4/10/25	5/10/15	0.6 mm	20	

Table 3a Specification of the linear incremental magnetic position/distance sensors. System error is calculated for the industrial temperature range and includes also the scale.

Type	Pulses per revolution	Max speed	Code wheel
Baumer MGHP	524 288	10 000 rpm	internal
Baumer ITD	8 192	5 000 rpm	External, tape
Exxelia IME15	262 144	2 000 rpm	internal
Siko MSA	64 000	32 m/s	External, 1 mm distance

Table 3b Specification of the angular incremental magnetic position sensors

2.5.2. Absolute encoders (incl Vernier and pseudorandom code)

Classical absolute encoders use multiple tracks coded in Gray code to avoid gross error during logical hazards. Using the nonius (Vernier) principle [34], an absolute encoder can be constructed with only two magnetic tracks: 19-bit resolution (equivalent to 2.5 arc seconds) is obtained for rotation speeds up to 11 000 rpm. A combined magnetic rotational encoder, 67.11 mm in diameter (including the shaft) and 6.9 mm in thickness, has a precision of ±6', comparable with a 15-bit photoelectric encoder, and static resolution of ±0.6′ [8]. Absolute magnetic encoder based on eddy currents in conducting non-magnetic code disk suffers from high sensitivity to manufacturing tolerances [35].

Another technique for the absolute position sensing is using a single track with a pseudorandom code sequence and a linear sensor array aligned in the direction of the motion [36]. Using this principle together with interpolated incremental track, a 26-bit linear position sensor with 0.244 μm resolutions was constructed by RLS company [37]. The most popular sensors used for magnetic encoders are AMR, but TMR (SDT) devices have large potential due to their small size and thus high spatial resolution. Using the separate incremental track is not possible in the case that the sensor geometry is rotational and a magnetic scale is made on

the rod which may rotate with respect to the sensorial part. The synchronization method proposed by Denic and Miljkovic elegantly solves this problem by using the Manchester code. Using their method, the single track scale can be simultaneously used for absolute position sensing, synchronization, and interpolation [36].

3. Eddy current position sensors [27]

Eddy current position sensors are also called **inductive or inductance sensors**. Their target should be electrically conducting, but not necessarily ferromagnetic. In this, they differ from variable gap sensors, which measure the displacement of the ferromagnetic part of an AC magnetic circuit. Eddy current-based instruments measure displacement, alignment, dimensions, vibrations, speed, and also identify and sort metal parts in industrial applications. Eddy current sensors have no lower limit on target speed. The principles utilized in conventional eddy current (inductive) proximity and linear distance sensors are explained in [38]. New types of eddy current sensors with nanometer resolution are described in [6].

AC magnetic field is created by the sensor coil supplied by an oscillator or generator. The coil is often tuned by a parallel capacitor and the LC circuit oscillates at the resonant frequency. If the conducting target is present, the eddy currents (mostly close to the target surface) create a secondary magnetic field decreasing the coil flux and thus the coil inductance. The sensor sensitivity depends on the target conductivity. An excellent target is aluminum; the recommended thickness is > 0.3 mm and a diameter of 2.5 to 3 times the diameter of the sensor coil [39]. In any case, the target thickness should be significantly larger than the skin depth δ

$$\boldsymbol{\delta = \frac{1}{\sqrt{0.5\omega\mu\varrho}}} \qquad \textbf{(1)}$$

where σ is electrical conductivity

μ is magnetic permeability

and ω is angular frequency

In the case of the ferromagnetic target, the situation is complicated, as the coil inductance is

simultaneously increased by the target permeability $\mu > 1$. **Fig. 11** shows the relative eddy current output for various target materials.

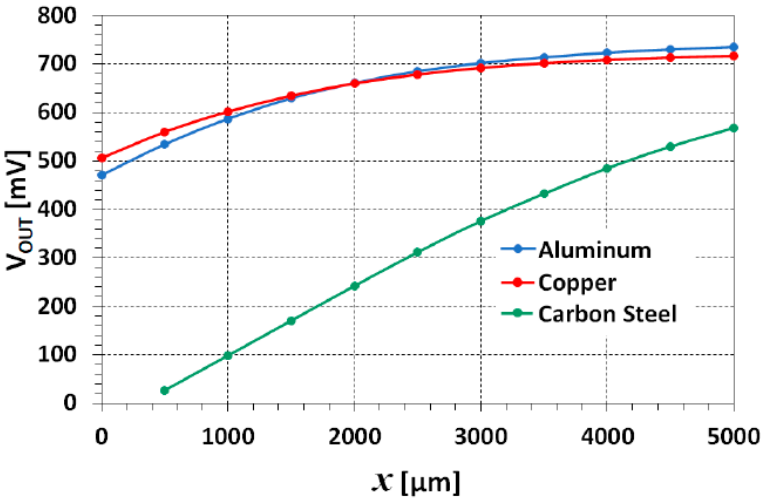

Fig. 11: Influence of the target material on the sensitivity of the eddy-current sensor – reprinted from [40] under CC BY licence.

Because of the complex dependence on the target geometry and material, the position measuring system should usually be individually calibrated. For ferromagnetic targets, we may expect increased sensitivity to target axial displacement, to temperature changes, and also worse repeatability and long-term stability. On the other hand, ferromagnetic targets increase the measuring range. The usual measuring range is up to 30% of the coil diameter. A lower range of 5 % or 10 % coil diameter is recommended for high-precision measurements, while in low-accuracy (for example switching) applications the range can be more than 50 % of the coil diameter. In any case, the minimum coil-to-target distance is usually 10 % of the range; this distance is often defined by the thickness of the sensor housing.

The sensing coils are often accompanied by a ferromagnetic circuit, which focuses their AC field in one direction so that the sensor is insensitive to conducting materials from the side or the back. The working frequencies range from kHz to 1 MHz, the core material is usually ferrite, and the typical shape is pot core (Fig. 12).

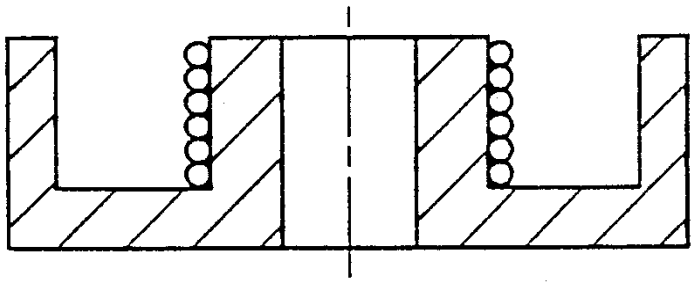

Fig. 12 Standard pot core used for eddy-current sensors. The diameter of this core is 22 mm, height 6.7 mm – from [41], © 1997 IEEE

The sensor diameter ranges from 8 mm to 150 mm with sensing distances between about 2 mm and 100 mm. The analytical solution of eddy current sensors is complicated, finite element modeling (FEM) software packages are being used. Improved core shapes are shown in Fig. 13. Fig. 14 shows the measured Q factors of the 47 turn coils wound on cores from Fig. 12 and Fig. 13 at the 300 kHz frequency, versus the target distance [41]. It was shown that the flat face of the transducer increases the value of B in the axial direction. The larger radiating surface increased the measuring range up to double the value of the potcore. Magnetic short circuits by the core itself or by ferromagnetic housing should be avoided. Eddy-current sensors working at higher frequencies should be wound from litz (stranded) wire.

The sensors work either in FM mode when the oscillator frequency changes with target position (relaxation oscillator) or in AM mode when the variable is the oscillator amplitude.

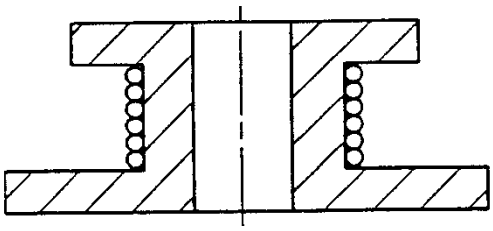

Sample 1

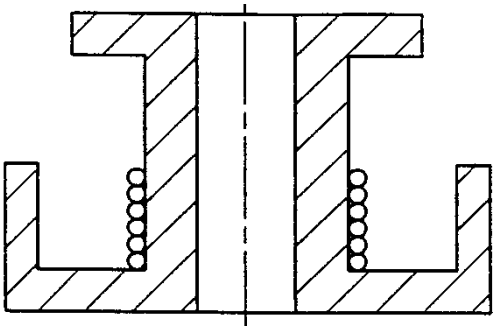

Sample 2

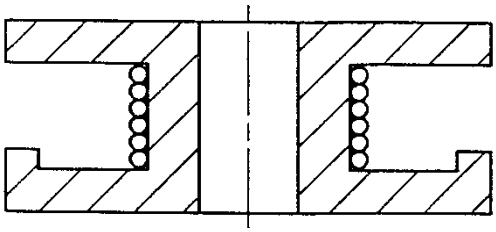

Sample 3

Fig. 13: Alternative shapes of ferrite cores for eddy-current sensors – from [41], © 1997 IEEE

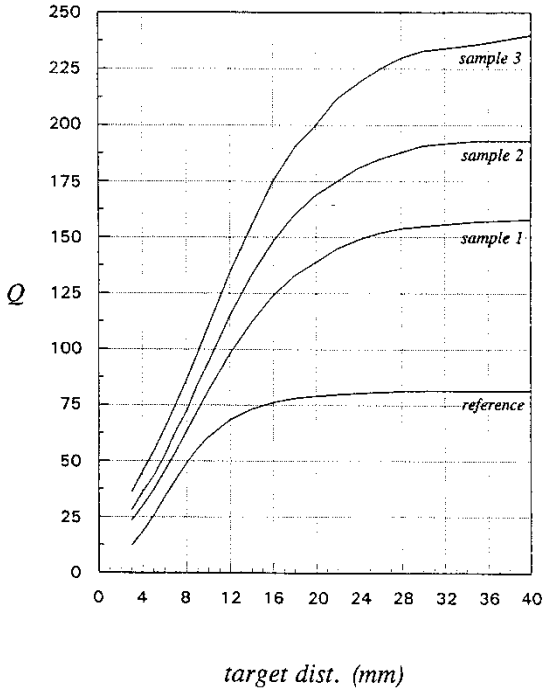

Fig. 14: Measured Q for reference pot (Fig. 12) and alternative cores (Fig. 13) - from [41], © 1997 IEEE

This principle is also often used in bipolar-output proximity switches – in this case, the electronics may be much simpler. The most popular type of eddy-current proximity switch is "the killed oscillator" (also "blocking oscillator"): metallic object moving close to the coil decreases the quality factor of the coil, which decreases the oscillator amplitude or, which stops the oscillation.

Miniature eddy current sensors use flat air coils. The proximity sensor based on a differential relaxation oscillator (Fig. 15) was described in [42]. The oscillator frequency changes with the position of the target. 1x1 mm coil on top of integrated CMOS readout circuit was developed for short-range applications with limited accuracy. 3.8 mm side coil temperature compensated sensor is working in the 3 to 4.5 MHz output frequency range. The dependence of the output frequency on the distance of the aluminum target before and after temperature compensation is shown in Fig. 16. The measured distance of the aluminum target changes with temperature by less than +/- 1% (for aluminum target 1 mm from the sensor) in the whole –20 ^{0}C to + 80 ^{0}C industrial temperature range.

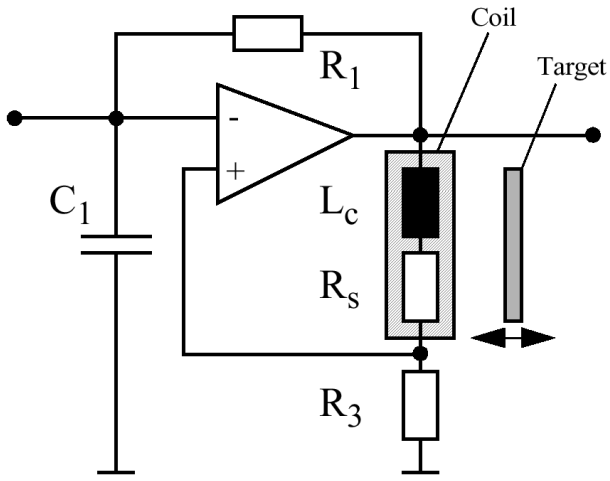

Fig. 15: Inductive (eddy current)proximity sensor based on differential relaxation oscillator. The output frequency is a function of the conducting target position – from [42].

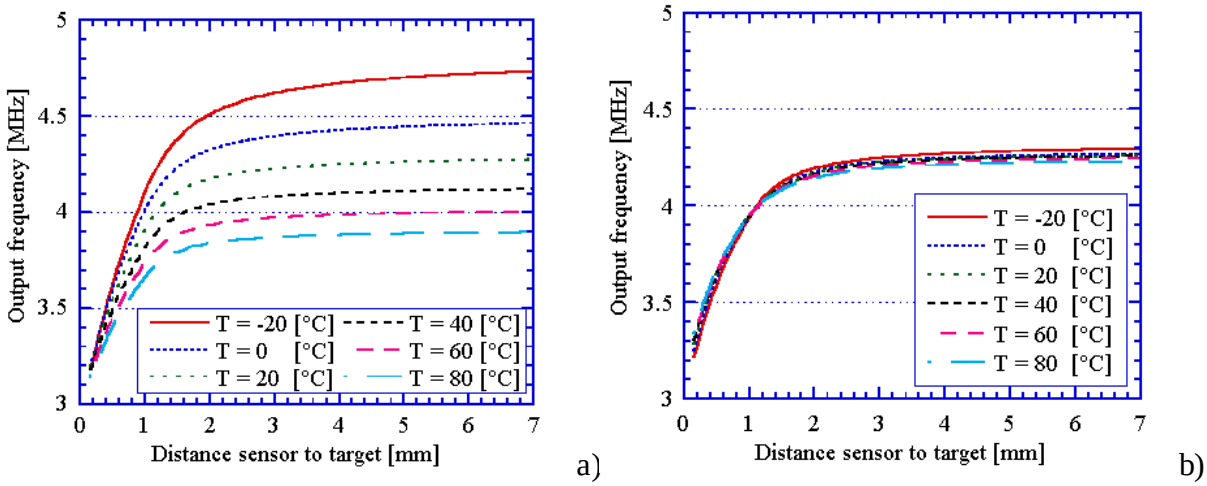

Fig. 16: Output frequency of the integrated inductive (eddy current) proximity sensor as a function of the distance of the aluminum target at various temperatures a)before and b) after temperature compensation – from [42].

The achievable range of the integrated eddy current proximity sensor is limited by the quality factor of the flat coil, which depends on the coil resistance. Conductor path resolution of screen printed thick film coils is limited to approximately 80 µm and maximum thickness is 10 µm. A molding of the sensor coil layout into a ceramic multilayer substrate via embossing combined with a photolithographic process was shown to increase the coil quality factor by a factor of 2.4. The sensitivity of an eddy current sensor with an enlarged conductor path cross-section is more than doubled in comparison with a screen printed coil with the same planar dimensions [43]

Eddy current microfabricated proximity sensors can be vertically integrated with capacitance sensors, keeping the sensing pixel small; while the conductive objects can be detected in long distance by an inductive method, plastic objects can be detected by capacitance method [44].

Low-cost eddy-current displacement sensors can be produced in PCB technology. A useful design case is shown in [45]. The working frequency of these sensors is 1 to 10 MHz.

In some designs the detector induction coil is replaced with a DC magnetic sensor, typically . an AMR magnetoresistor. While the sensitivity of induction coils increases with frequency, the sensitivity of AMR sensors is frequency independent. This allows the use of low-frequencies that can penetrate the metal wall of a pneumatic cylinder or barrel. AMR sensors are also sensitive and small which results in higher spatial resolution. It is also easy to built AMR sensor arrays.

If the AC excitation and flipping frequencies of the AMR sensors are the same, the magnetoresistor has DC output without any demodulator [46]. .

The main drawback of eddy current position sensors is that their sensitivity depends on conductivity, permeability, and size of the target. Replacing an induction coil by a DC magnetic sensor allows to distinguish ferromagnetic and non-magnetic targets. The dependence on the target thickness can be suppressed by using a high enough excitation frequency, for which the penetration depth is significantly smaller than the minimum thickness of the target. In general, the eddy current distance sensors should be calibrated with each target.

High-precision eddy current sensors utilize compensation of temperature dependence and nonlinearity by microprocessor or FPGA circuit. Table 4 shows parameters of some of these devices.

type	Min range (mm)	Max range (mm)	Resolution (nm)	Drift (%FS/K)	Linearity (%FS)
Lion Precission U3	0.05	0.25	10	0.08	0.2
Lion Precission U50	2	15	300	0.02	0.2
με eddyNCDT 3300 ES04	0.04	0.4	40	0.015	0.2
με eddyNCDT 3300 EU80	8	80	4000	0.015	0.2
Kaman KD-510020N	0	1.9	100	0.025	10
Kaman KD-230660U1	0	60	6000	0.02	1

Table 4 Specification of the precise inductive distance sensors -from [4]. FS is a full scale (range) of the sensor

Eddy current speed sensors

These sensors can be used to measure the speed of conduction objects without teeth [4].

An eddy current speed sensor based on a permanent magnet and a Hall sensor was described in [47]. The sensitive axis of the Hall sensor is oriented orthogonally to the field of the magnet, so the sensor output is zero for zero speed. When the conducting target moves, eddy currents are generated in it, and magnetic field associated with these eddy currents can be sensed by the Hall sensor. The sensor has several disadvantages that prevented its industrial applications: temperature offset drift of the Hall sensor, sensitivity to external magnetic fields, and poor long-term stability due to sensitivity to angular errors between the excitation coil and sensor.

A novel eddy current linear speed sensor allows to measure speed of an iron rod. It has applications in linear machines and pneumatic and hydraulic cylinders [48]. Instead of a permanent magnet, the system uses an AC excitation coil. The motion eddy currents are sensed by two antiserially connected pick-up coils (Figure 17). For zero speed the magnetic field is symmetrical so that the output voltage is zero. This symmetry is broken due to the motion eddy currents (Figure 18) and the differential output voltage depends linearly to the speed. For 20 mm diameter iron shaft and 47 turns of all coils, the sensitivity was 150 μV/ (m/s), resolution was 10^{-3} m/s in the 10 Hz and the linearity error is 0.4 % (Figure 19).

The excitation and sensing coils can be also perpendicular to the movement speed. .A flat sensor of such design has rectangular coils. The moving target is external to the coil. Such setup may serve e.g. for the measurement of vehicle speed with respect to the conductive rail [49]. Typical sensitivity of 100 μV/ (m/s) and resolution of $2 \cdot 10^{-3}$ m/s in the 10 Hz bandwidth can be achieved with 100-turn coils. The sensitivity can be increased by using higher excitation frequency, but increasing the operating frequency decreases the skin depth and

increases the sensitivity to the surface properties of the armature. Temperature compensation and compensation of the lift-off can be made by the ratiometric method using voltages of the individual output coils.

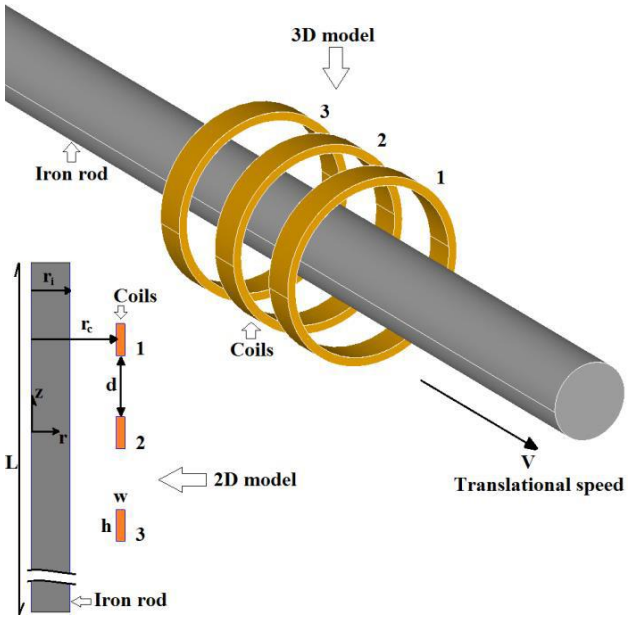

Figure 17. A coaxial eddy current linear speed sensor: sensor configuration with excitation coil in the middle and two sensing coil which are connected antiserially. For the developed demonstrator w = 1.8 mm, h = 5 mm, d = 10 mm, and r = 10 mm. © 2019 IEEE Reproduced from [48] with the permission of IEEE.

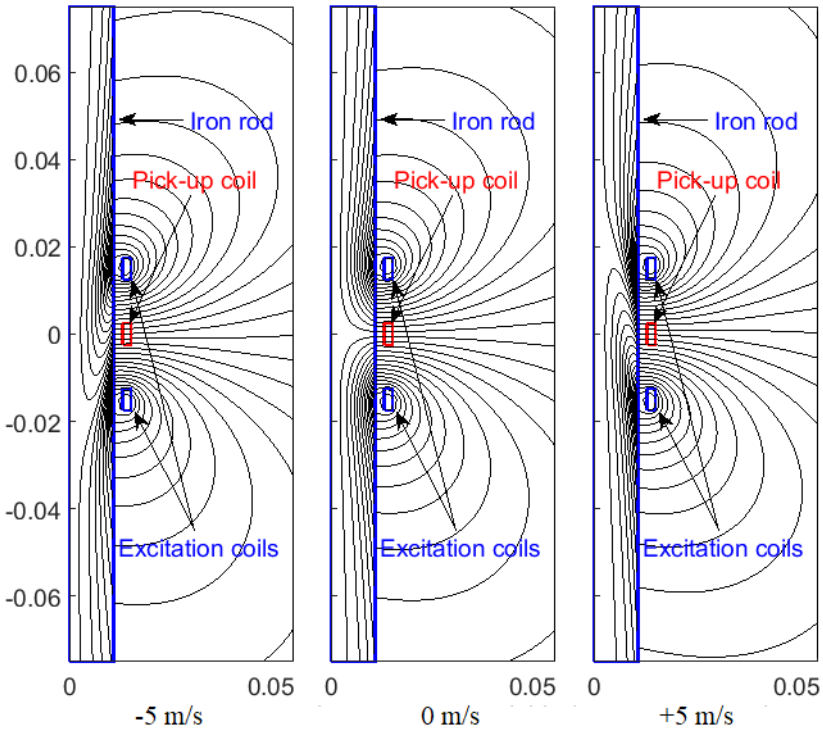

Fig. 18. A coaxial eddy current linear speed sensor: magnetic field distribution at zero speed and at a speed of +/- 5 m/s. The solid iron rod has a relative permeability of 77 and conductivity of 4.45 MS/m. From [4]

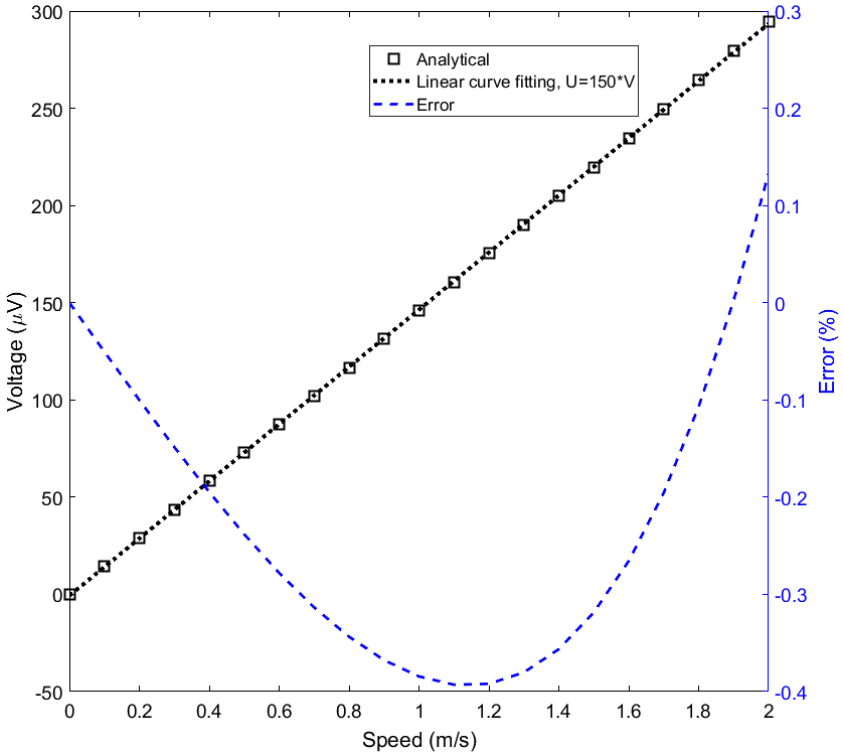

Fig. 19. Characteristics and linearity error of the eddy current speed sensor. The analytical calculation assumes a low magnetic field and thus constant initial permeability of the iron rod. Linearity relative error was calculated as %FS (full scale). From [4].

4. Transformer and inductance sensors [1,4]

4.1 Linear transformer and inductance sensors

A simple linear position sensor uses dependence of the solenoid inductance on the position of movable core. The sensor linearity can be improved by adding more turns at the coil ends [50]. The disadvantage of this simple sensor is its large temperature dependence. Transformer sensors have two windings, but effective temperature compensation can be made using the ratiometric method.

LVDT

Linear Variable Differential Transformer (LVDT) is probably the most popular magnetic position sensor. Because of zero friction, the device is highly reliable. It has one primary (excitation) and two secondary windings (sensing) coaxial coils and movable ferromagnetic core (Fig. 20). While the textbooks usually show separated primary and secondary coils, in practical devices these coils partly overlap in order to compensate the nonlinearity.

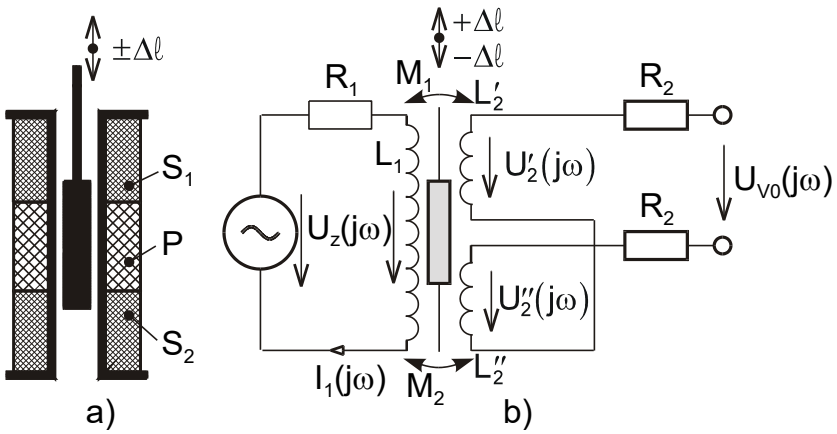

Fig. 20 LVDT sensor

LVDT sensors have high reproducibility, practical resolution may be better than 0.1 % or below 1 μm, linearity up to 0.05 %, temperature coefficient of sensitivity is typically 100 ppm/^{0}C. The linear range is 30 % to 85 % of the device length. Standard measurement ranges are from 200 μm to 50 cm. The excitation frequency is usually between 50 Hz and 20 kHz. Basic design considerations for LVDTs are given in [51].

The output signal of LVDT sensors is often processed by PSD (phase-sensitive detector = synchronous rectifier, lock-in amplifier), but ratiometric processing is used more often [52, 53]. Synchronous demodulation is less noisy and is more resistant against interference, but requires phase corrections. Other less utilized methods include Dual Slope conversion [54] and position to frequency converters based on relaxation oscillator [55] or Colpitts LC oscillator [53]. All these methods are simple and fast, but they have higher linearity errors.

LVDT signal conditioner including all phase corrections can be also programmed in FPGA resulting in comparable error with monolithic and processor-based signal conditioners but with faster response [56]

It is possible to integrate the complete sensor electronics including the excitation generator into the sensor housing. Specialized integrated circuits such as AD698 and the NE5521D (based on demodulator) are available [51].

LVDT can be easily temperature compensated using ratiometric method. 0.15% error in a wide temperature range is achievable [57]. LVDT linearity can be significantly improved by coil design – proper profiling of the secondary coils and their overlap can increase the linearity range significantly. Another method to improve the linearity is by signal processing [58, 59]; analog technique based on the inverse transfer characteristic of the LVDT generated by the analog multipliers and the difference amplifier proposed in [60, 61] achieved 0.07 % linearity error. The inverse model used for the correction can be trained by a simple neural network [58].

The differential variable inductance transducer (DVRT ®, "half-bridge LVDT") has only two windings; core position is measured by differential inductance. DVRT sensors with 1.5 mm outside diameter and 60 nm resolution are available. Sensors of this type can measure the position of the ferromagnetic piston disk inside the ferromagnetic cylinder. The linear range is 100 % of the 200 mm stroke and the maximum linearity error was 20 μm [62]. A similar sensor for nonmetallic hydraulic cylinders was using an aluminum core, which exhibits zero hysteresis error [63].

An LVDT can be magnetically shielded for operation in large disturbing magnetic fields [64]. Inductive position sensor with moving coils instead of ferromagnetic core for high radiation environment is described in [65]. Similar sensor using two coils with inductance-to-voltage converters is described in [62].

The standard material for the LVDT sensor core is ferrite, FeNi materials are used at low-temperatures at which would ferrites failed [66]. Very small LVDT sensors were designed with core made of amorphous wire [67, 68].

The basic ratiometric temperature compensation provides 0.15 % error in a wide temperature range [60], with temperature coefficient below 100 ppm/K. LVDT sensors with 0.1 % linearity are commercially available . The linear range of LVDT can be further extended by digital compensation. Extension from 4 mm to 30 mm stroke was reported in [61] while linearity error was only 0.07 %.

A transformer position sensor was also designed to measure the position of the piston in a pneumatic or hydraulic cylinder. In this case the ferromagnetic piston rod serves as a moving core, and the coils are wound on top of conducting cylinder. The excitation field should have low frequency so that it is only partly attenuated by the cylinder wall [69].

While the common LVDT sensors are cylindrical with solenoid coils and moving rod core, flat devices are required for some applications. A planar design using flat coils was described in [70] and [71], but these devices used a moving coil, which is unpractical especially for long sensors. We have designed a flat position sensor with stationary coils and a moving ferromagnetic armature (Fig.21]. This type of sensor can have a multiple coil sets to extend the detection range: a typical application of such configuration is as a cabin landing sensor for elevators: the single armature is connected to the cabin and one set of coils is located on each floor to measure the cabin landing position with high accuracy. For 70 mm long coil set, 0.25 mm error without any compensation was achieved in a ±20 mm range (Fig. 22)

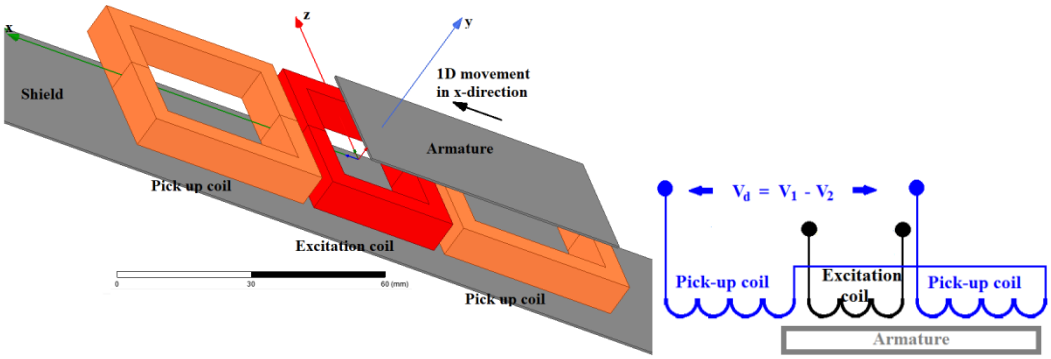

Fig. 21 A flat linear transformer sensor consisting of a stationary coil set with ferromagnetic shielding and moving armature - from [4]

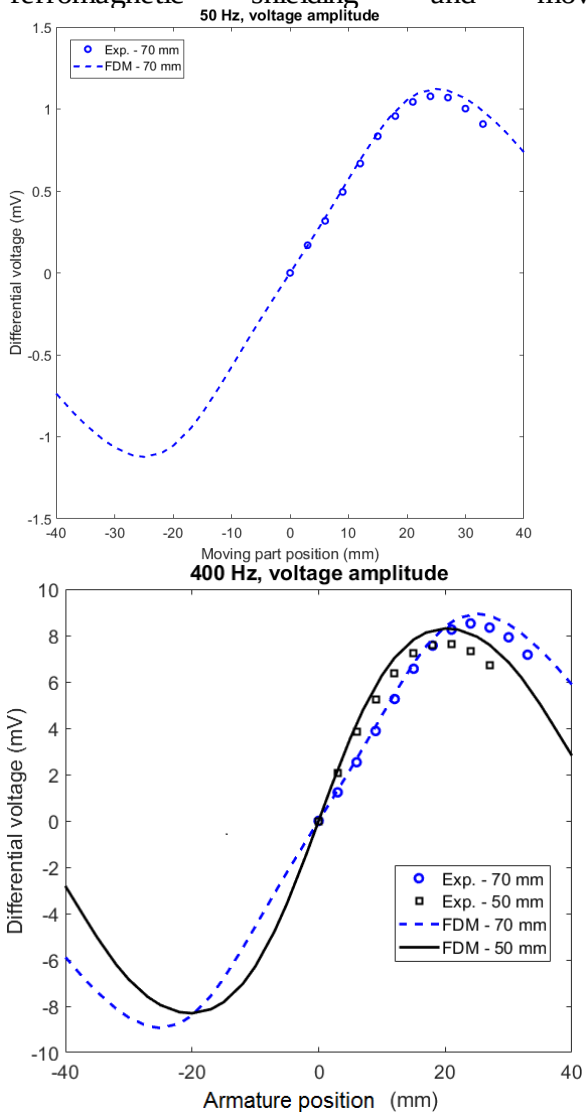

Fig. 22 Differential voltage versus steel lamination armature position – a) at f_{exc} = 50 Hz and b) 400 Hz Experimental results (Exp) versus calculations by finite-difference method (FDM). 2-D FDM is a fast calculation method suitable for sensor optimization.. - from [4]

A similar configuration on a small scale was used in the integrated position sensor which combines linear encoder with LVDT. The scale is cut from transformer steel and two transformer pairs with flat coils are made in PCB technology. The achieved resolution is 20 μm for 4 MHz working frequency [72].

LVDT can be made radiation-resistant up to 50 MGy if proper isolation and sealing materials are used. The conditioning electronics should be taken away from the radiation zone. The cable length can reach hundreds of meters if special reading techniques are used. However, LVDT is sensitive to magnetic fields in the axial direction, which may cause drifts. The problem is caused by the presence of non-linear magnetic materials. An ironless position sensor was developed for installations with high magnetic interference. It consists of two solenoid primary coils, a short-circuited secondary moving coil, and a pair of sense coils. [73]. The moving coil acts as a shielding which decreases the inductive coupling between primary and sense coils. This is similar to the performance of the solid piston rod in the transformer sensor of the piston position for hydraulic cylinders reported in [74].

Inductosyn and similar devices

Inductosyn ® [75] is a classical device that is still in use for some military and industrial applications. It consists of two parallel flat meander coils: scale and slider. The slider usually has two windings ("sine" and "cosine") shifted by 1/4 of the mechanical period (pitch). Inductive coupling between scale and slider coils measures the displacement. Inductosyn combines the advantages of incremental sensors (the increment is one pitch) and analog sensors (sinewave dependence of the output voltage allows to interpolate the fine position with a resolution of up to pitch/65 000). The scale winding is usually supplied by AC of typically 10 kHz frequency, and the voltages induced in sine and cosine slider coils are

processed; however, it is also possible to supply the slider sine and cosine coils by quadrature (sine and cosine) voltages and to process the voltage induced in the ruler ("stator") coil. The standard pitch size is 2 mm, ruler length may range from 25 cm up to 36 m or more.

Inductosyns are also made rotary. Multiple patterns can be combined in one device in order to increase the incremental resolution by employing techniques known from optical encoders (such as the N/N-1 method).

A large group of inductive position sensors is using flat coils made by printed circuit board (PCB) technology and flat ferromagnetic parts with different shapes [76]. Improved design with a U-shaped core around the PCB has a resolution of 6 μm and 80 mm stroke. The stroke can be increased without limitations by repeating the coil motive. Thanks to the design, the inductance vs. position dependence are precise sinewave so that signal processing is easy. Without any correction, the achieved error was 0.2 % [77].

4.2 Rotational transformers

Rotation transformer position sensors

Although rotation transformers are sometimes considered to be archaic devices, they still find application in extreme conditions, as they are more rugged than optical encoders.

Synchros

Synchros are electromechanical devices, which replicate the rotor position in a distant location. They have three stator windings displaced by 110^0. They combine the properties of sensor and actuator; the typical application is the antenna rotator.

Resolvers

Resolvers have windings displaced by 90^0 [78]. There are different types of resolvers including wound rotor resolvers, variable air-gap length variable reluctance resolvers, and sinusoidal rotor variable reluctance resolvers. The outputs are sine and cosine voltages, which are often processed by specialized resolver-to-digital converters [79-81]. Brushless resolvers use another rotational transformer to supply the rotor [82]. Resolvers can be made to withstand temperatures from 20 K to 500 K, radiation of 10^9 rads, acceleration of 200 g (battleship cannons, punching devices), vacuum, or extreme pressures. Their disadvantage is a large size and weight. The design of resolver based on Finite element analysis is described in [83].

Some manufacturers (e.g. Pewatron) use the term "Linear resolver" for linear position sensors that also have Sin/cos outputs, but which are based on two AC supplied magnetoresistive elements.

Another type of rotation transformer with an air core is the rotational version of Inductosyn.

5. Variable gap sensors

Variable gap (sometimes also "variable reluctance") sensors are based on the change of the airgap in a magnetic circuit (between core and armature) of the inductor or transformer. These sensors are still described in textbooks, as their principles and methods of linearization are quite didactic. However they are less precise than LVDTs, and currently, they are rarely used for new designs.

The term “variable reluctance” is sometimes also used for DC sensors energized by stationary permanent magnets which sense salient soft magnetic object such as a toothed wheel. This type of sensor is described in Section 2.

Mutual inductance of two coils depends on their distance. Sensors based on this principle can be very small: the microfabricated 1x1 mm device achieved 17 nm resolution and 0.15 % hysteresis [84]. Sensors of this type with a range of up to 20 m are described in Section 7.

Simple variable reluctance linear position sensors energized by permanent magnets and using Hall sensor as detectors achieved linearity of ±1 % [85]. The advantage of this type of sensor is that the magnetic sensor is partly shielded from external interference.

6. Magnetostrictive position sensors

Magnetostrictive position sensors measure the time of flight of a strain pulse to sense a position of moving permanent magnet (Fig. 23). The sensing element is a wire or pipe from magnetostrictive material (sonic waveguide). The devices are based on the Wiedeman effect: if the current passes through the waveguide and a perpendicular DC magnetic field is present, the torsional force is exerted on the waveguide.

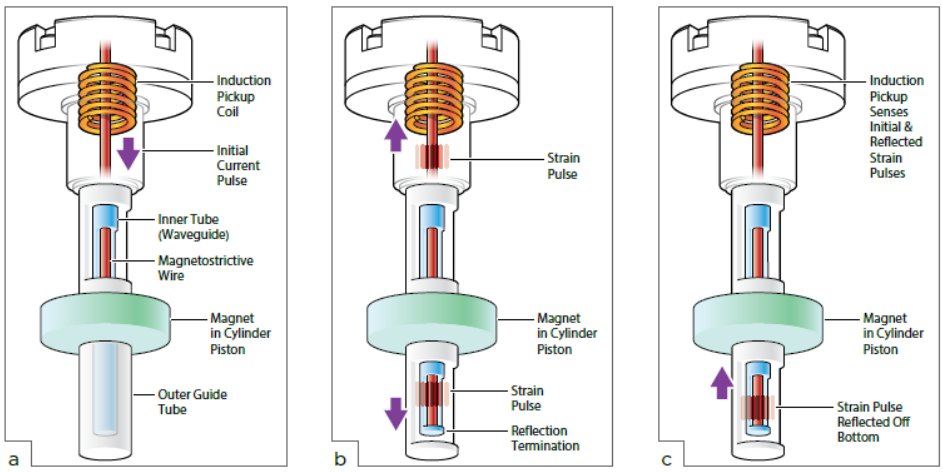

Fig. 23 Magnetostrictive position transducer. Image is courtesy of AMETEK Sensor Technologies.

The device works so that after the current pulse is applied, the torsional force is generated in the location of a permanent magnet. This torsional strain pulse travels with ~3 km/s speed along the waveguide and it is detected by the small induction coil at the sensor head. The hysteresis may be as low as 0.4 μm, uncorrected linearity is 0.02 % FS, some devices have an internal linearization and temperature compensation. The maximum sensor length is limited by elastic wave attenuation to about 4 m [86, 87]. Sensors based on similar principles are manufactured by Gemco-Patriot, MTS, and Balluff.

Other devices based on a delay line principle were suggested in [88, 89]. The mechanical strain in the delay line is caused by a current pulse in the perpendicular movable conductor.

This momentary strain induces surface acoustic wave which propagates in both directions. The acoustic pulse is again detected in a small axial induction coil close to the end of the delay line due to the inverse magnetostriction effect. The delay line position sensors have an error of approximately 1 mm, so they may be suitable to measure distances of about 1 m to 5 m the upper limit being determined by attenuation. The magnetostrictive response of the amorphous wire used as a sensor core was optimized by stress annealing [90].

A similar configuration was used in a 2 m long sensor and the achieved error was 30 μm. [86]. Parameters of some commercially available devices are summarized in table 5.

type	Min range (mm)	Max range (mm)	Resolution (μm)	tempco	Linearity
Festo MME-MTS	225	2 000	10	15 ppm/K	0.002 % min ±50 μm
Baluff BTL 7	25	7620	5		± 30 μm
Ametek Patriot Vmax	300	5 000	1 or 5		< 0.01 %

Table 5 Specification of the magnetostrictive linear position sensors

Magnetostrictive position sensors can simultaneously measure velocity by the eddy current principle. The independent velocity information can be used for consistency checking (self-diagnostics), or the improvement of the position measurement by signal fusion [91] [87]. Some attempts were made to utilize domain wall movement for the position measurement, but this effect is too dependent to external magnetic field and stress.

7. Long-range position sensors and magnetic trackers

Magnetic compass

The magnetic compass is using the Earth's magnetic field to evaluate azimuth. When the compass magnetized needle is kept in the horizontal plane, it points to the magnetic North. The electronics compass uses a tri-axial magnetometer and inclination sensors. Pitch and roll

angles measured by inclinometers are used to rotate the measured magnetic field vector to the horizontal plane and subsequently, the azimuth can be calculated. Magnetic sensors used in the precise compass are fluxgates, which allow precision of several angular minutes. Magnetooresistors are used for mass market devices such as mobile phones or smart watches; the achievable error is 2°.

A compass should be calibrated for the errors of the magnetometer: uneven sensitivities of individual axes, angular deviations, and offsets, both of the magnetometers and inclinometers. This calibration is made before the compass is mounted on the platform. The calibration procedures are either vectorial or scalar. Vectorial methods using Earth's field are based on the precise rotation of the sensor using a non-magnetic platform [92] and also in [93, 94]. Another method of vectorial calibration of the magnetometer is using a precise 3-axial axial coil system; inclinometers naturally cannot be calibrated [95], [96]. Scalar calibration is a statistical procedure that does not need precise positioning - it is based on random positioning in a stable and known magnetic field [97]. The procedure can be automated by using a non-magnetic positioning platform [98]. While for calibration of the magnetometer 2-axial positioning system is sufficient, full calibration of compass requires all 3 positioning axes. [99]. An alternative scalar calibration procedure is called a thin shell and it is based on a stable sensor and rotating magnetic field created by a precise coil system [100]. Again, the thin shell method can be used only for magnetometers, not for inclinometers.

After the compass is mounted on the platform, other disturbances appear, which rotate with the platform. They are divided into hard iron disturbances, which are created by permanently magnetized elements, and soft iron disturbances, which are caused by objects with magnetic permeability not equal to one. These internal disturbances can be compensated by proper calibration procedures which are usually based on rotation around their axes [101, 102]. External disturbances can be neither estimated, nor corrected. They come from

unpredictable external sources, however, their influence can be suppressed by using Kalman filters which identify and reject corrupted measurements [103].

Magnetic compass, inclinometers, and angular rate sensors are the main components of the inertial navigation systems (INS) or inertial measurement units (IMU). Cheap small-size IMUs are part of many smartphones. They can serve also as indoor localization systems using fingerprint database magnetic map [104] [105-107]. One of the successful methods for error correction for indoor navigation is using dominant orthogonal directions of corridors in buildings [108]. Some systems also use magnetic landmarks made of permanent magnets or magnetic beacons [105, 109, 110].

Inertial measurement units can also be used for other applications such as monitoring the position of a needle during surgery, with an achievable position mean error of 1.3 mm [111].

Magnetic trackers

Trackers are devices that measure the location and relative orientation of the target. A complete tracker has 6 degrees of freedom (linear position in 3 axes and 3 rotation angles). The applications include body tracking in virtual reality, motion capture in animation and biomechanical measurement, indoor navigation and security [112] [113]. Miniaturized sensors are used to locate the position of probes and instruments such as biopsy needles inside the body, for surgery navigation, and for the location of the capsule in the gastrointestinal system [114, 115]. The target may be a source of the signal (permanent magnet or transmitter coil) whose amplitude (and eventually phase) is sensed by receiving coils, or the sensor is attached to the target. Passive systems with permanent magnet suffer from noise and drift caused by ambient magnetic fields. Within a 380×270×240 mm covered by 16 triaxial AMR magnetometers the average positioning error obtained from the proposed noise and drift cancelation algorithm is around 10 mm and the average orientation error is around 12°[116].

The simplest type of transmitting target is a small permanent magnet. Such systems have been used for observing bio-mechanical movements [117, 118] [119] and for non-contact joystick [120]. The position of the 1 mm long helical microrobot which contains a NdFeB permanent magnet is sensed by an array of 16 Hall sensors in the presence of the large field of rotating permanent used to actuate the robot. The microrobots are designed to remove superficial blood clots inside veins. For the distance of 3 mm between the robot trajectory and sensor array, the mean absolute error is 2 mm [121].

The limitation of using a permanent magnet as the field source is small range: an absolute position and orientation error of 71 μm and 1.4 deg are achieved with an array of 16*16 Hall sensors in 7 mm distance [120]. Motion capture systems using permanent magnets and fluxgate or AMR magnetometers may have a range up to 1 meter, but with limited accuracy. If the permanent magnets in 1 m intervals are used as markers for an automatically guided vehicle, the error of position estimate is ± 5 cm [122]. Chan presented an overview of algorithms applicable to the sensing of magnets and their application for vehicle guidance [123].

LC resonant target is truly wireless but if it is used for position tracking, the resulting uncertainty is 2 mm in the 60 mm distance. Similar targets are used as security labels for shops and libraries [124, 125].

Magnetic trackers with a sensing target consist of a transmitting coil (which may be flat) and miniature sensors (usually induction coils or magnetoresistors) attached to the target. The most popular configuration is using three orthogonal generator coils and a three-axial sensor [126, 127]. A closed-form solution for the general case of any directions of the coils and sensor axes is described in [128]. The tracker error may be 1 mm and 0.5^0 within a 1 m^3 volume [129]. The sensor signal may be wirelessly transmitted to the control unit. Some systems use a pulsed DC magnetic field instead of an AC field, and sample the position after

the decay of eddy currents; this technique reduces the errors caused by conducting objects. The accuracy in a large area can be increased by using multiple source coils [114]. Other systems are using a tri-axial magnetoresistive sensor attached to the target. Using DC magnetic sensors allows to combine compass with AC source: such a system is using only uniaxial transmitting coil. With a 16 mm diameter transmitting coil the tracking distance for 2 mm uncertainty is 100 mm [130].

Advanced tracking systems for biomechanics fuse signals from inertial sensors, magnetometers, and optical sensors [131]. A 6 degree-of-freedom (DOF: 3 for position and 3 for orientation) wearable multisensory tracking system for virtual reality is described in [132]. This system is fusing data from an infrared optical tracker with a low-cost camera and an inertial and magnetic measurement unit. The hand posture can be tracked with a 0.2 mm position error.

A 5-DOF (without roll) indoor magnetic positioning system based on a single transmitting coil mounted on a moving object and three tri-axial magnetic sensors is described in [112]. The achieved error is 10 cm and 6 deg.

Applications of magnetic tracking in medicine include bronchoscopy, punctures, intubation, and other surgery, sonography, radiotherapy, and catheterization. Systems manufactured by Northern Digital, Ascension Technology, Biosense Webster, Polhemus, Medtronic, and other companies are described in an excellent review by Franz [133].

Another application of magnetic trackers is underground drilling. These systems utilize compass, active beacons, and inertial sensors, as only sensor fusion can provide the required accuracy [134].

An example of an underground positioning system is shown in [135]. The gyro is used for dead-reckoning navigation over kilometer-long distances. A magnetic tracking system

consisting of two coaxial solenoid transmitters and two tri-axial magnetometer receivers is used when two drilling heads approach each other. By using only longitudinal excitation field the direction and distance can be calculated from two 3-axial readings. The magnetic approaching system has a maximum range of 17 m with 1.2-m RMS uncertainty, which is sufficient to steer the drilling heads. The accuracy increases by using a larger number of the collected field data and also fast increases during the approach. At the distance of 10 m, the RMS error is only 0.34 m and the final approach is navigated with cm uncertainty. A less precise approaching system using a permanent magnet has a detection range of 3 m [136].

A navigation tool for low-diameter drilling in coal mines is using only a strapdown navigation unit (triaxial magnetometer and inclinometer) and odometer (for the measurement of the distance on the drilling path). The complete error model of the sensor head has 24 parameters: sensor sensitivities and offsets, nonorthogonality error, and misalignment with the platform. Incomplete calibration strategy during drilling is using unit rotation and allows to reduce path estimation errors [137]. Similar methods are being used in space research for in-flight calibration of magnetometers onboard spacecraft [99, 138, 139].

The Earth's magnetic field is distorted by underground ferromagnetic objects, including drilling pipes. This error can be reduced by repeated measurements and multiple sensors [140]. Systems for petroleum extraction require to drill multiple parallel holes. For this type of work, local magnetic field anomalies are also employed to increase accuracy [140].

Localization of metal objects is important topic, but it is out of the scope of this paper. Here we only mention several pplications. Conducting foreign objects in the human body can be localized by magnetic sensors [141]. Eddy current metal detectors are used to detect low-metal-content mines, and DC magnetic sensors are used to detect ferromagnetic objects from large distances [1] [142].

Long-range position and distance sensors are based on similar principles as magnetic trackers [143, 144]. A distance sensor consisting of two air coils is reported in [145]. The transmission coil is supplied by squarewave voltage and tuned by parallel capacitor. The position error is 1 % for a 240 mm range. Similar sensors with solenoid coils developed for biomagnetic applications are described in [146]. A tri-axial miniature sensing coil was used to correct for an angular mismatch between the transmitter and sensing coils. This sensor was developed to measure the gastric activity. The achieved measurement range was 120 mm with an uncertainty of 5% and resolution better than 1 mm. While such precision would not be unacceptable for industrial applications, it is sufficient for medical research.

Liu uses a rotational permanent magnet on the surface and a tri-axial magnetometer at the drilling head [147]. The sensing range was limited to 5 m because of the AMR sensors that were used, but the position error was only 2 %.

A precise distance sensor based on the principle of magnetic tracking is described in [148]. The system consists of a 35 mm long, 22/35 mm diameter tri-axial stationary excitation coil system and a moving precise Billingsley tri-axial fluxgate magnetometer.. The excitation coils are sequentially powered by bipolar current pulses. The selection of the excitation frequency is a compromise: high frequency system has fast response time, but it is more susceptible to errors due to eddy currents in conducting objects. The achievable precision is 1 % for arbitrary position and orientation. Using larger excitation field and more precise fluxgate sensors, the range can be extended up to 50 m.

Very large angular position sensors with 33 m diameter have been built for walking crane for surface coal mines. The device works in extreme conditions regarding temperature, vibrations, dust, and mud. The active magnetic source is mounted on the moving part and an array of 48 fluxgate sensors are attached to the static part [149]. The magnetic source soil e is a 60 cm long, 5 cm diameter solenoid powered by a 2.5 A/50 Hz sinewave. The distance

between the sensor and the field source is 1.5 m.

Another application of magnetic sensors in surface coal mines is the detection of ferromagnetic objects on conveyors transporting coal and soil. Using digital filtering and correlation techniques, the magnetic stray field of the object moving on a conveyor can be detected in the presence of strong interference [150].

DC and AC methods are being used for the detection and localization of mines, bombs, and unexploded ammunition [151]. An array of triaxial magnetometers has been used for the location and measurement of hidden electric currents [152].

An important application of magnetic position detection is in wireless power transfer. Transmitter and receiver coils should be aligned in order to increase efficiency and reduce magnetic field leakage, which can cause heating of metal objects in the vicinity of the wireless charger. For charging of electric vehicles, this can be achieved by using a set of auxiliary coils either on the primary or secondary side of the charger [153, 154]. For energy transmission systems for implant application, auxiliary coils were replaced by an array of TMR sensors on the transmitter side [155]. The array of 14×14 TMR sensors measure the coil position with the error of 3.7 mm and detect small and multiple magnetic objects in the vicinity of the transmission coil [156].

The walking detector was developed to find the position of a pig inside a ferromagnetic pipe [4]. The pig is equipped with a solenoid field source (beacon) as shown in Fig. 24. The solenoid has 3000 turns and 130 mm long, 20 mm diameter iron core. The inductance of the solenoid is 0.94 H and its resistance is 25 Ω. The solenoid is energized by a 180 mA/12.5 Hz current.

The working frequency is low to allow the beacon signal to pass through the metal pipe and also to limit field distortion due to eddy currents in other conducting bodies. Another requirement is that the working frequency should be far enough from the power line

frequency (50 or 60 Hz). The detector is a 200-turns pickup coil working in the short-circuited (current) output mode [157]. The detection limit is 1 nT corresponding to signal from a pig inside a steel gas pipe in the distance of 5 m. For plastic pipes, the pig can be detected from the distance of 8 m. The position error is 0.2 m due to the sharp minimum of the signal.

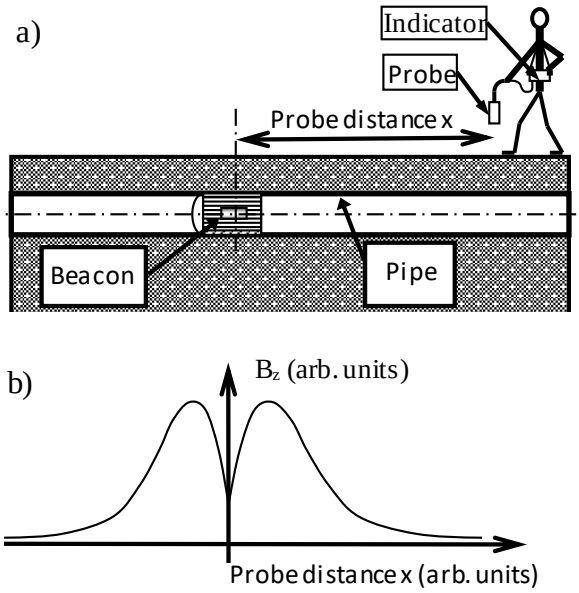

Fig. 23. A walking detector for a magnetic pig - after [4]: a) the beacon inside the pipe is a solenoid supplied with AC current, b) the vertical magnetic field component Bz as a function of the probe position x

Precise methods for long-range angular sensing based on solenoids are used in mining. A similar method was described for the measurement of angular misalignment of large coils in accelerators. Relying on a few measurements of the magnetic field by Hall sensors, this method is especially intended for applications where the magnet aperture is not accessible. The achievable uncertainty is 10^{-6} [158]

8. Trends and Conclusions

A large part of position sensors is based on magnetic principle as they are reliable and resistant and their price is competitive. Compared to optical sensors, magnetic sensors are

resistant to dust and oil and they do not require direct sight. Optical sensors may have a larger range. Capacitive sensors have the lowest range and highest precision.

Most of the magnetic sensors measure the position of an external target, which is either a permanent magnet, magnetic scale, ferromagnetic object, or just conductive metal (for eddy current sensors).

Sensors with permanent magnet have excellent resolution, but limited linearity. Limiting factor is also their sensitivity to external magnetic fields such as the Earth's field. The current development trend is therefore to replace permanent magnet by AC supplied coil on the stationary part.

For distance sensors based on magnetic scales the trend is to achieve absolute position sensing with minimum of tracks. Other magnetic position sensors such as LVDT measure the position of the core, which is a part of the sensor. New shapes of transformer position sensors are being developed to better serve industrial requirements on more compact devices.

PLCD sensors have a stable core which is magnetically cut into the two parts by saturation zone created by the moving permanent magnet. Although the precision of these devices is limited by their principle, they are robust and cheap and have stable position at the market. The saturated zone in magnetostrictive sensors reflects the elastic wave. These sensors are popular to measure distances up to 10 m with high precision. New temperature compensation methods are being developed to compensate even large temperature gradients.

Magnetic navigation systems and trackers utilize the Earth's magnetic field or artificial field generated by coil systems. They can achieve 0.1° angular error and 0.1 % position error, but their accuracy may be degraded by conducting objects which distort the magnetic field. Modern tracking systems use fusion of DC and AC magnetic and optical sensors to use the advantages of all principles.

Magnetic sensors used in position detectors are Hall sensors, inductive coils, and

magnetoresistors, namely AMR, GMR, and TMR. The other principles include GMI, transformer, and magnetostriction. Hall sensors still dominate in these application, as they were further developed to achieve better offset stability using spinning current method. AMR sensor are more often used due to their low noise which allows to decrease the source field or increase the distance between the field source and sensor.

Acknowledgement

This work was supported by the project Mobile Monitoring System for the Protection of Isolated and Vulnerable Population Groups against Spread of Viral Diseases, ITMS code 313011AUP1, co-funded by the European Regional Development Fund under the Operational Programme Integrated Infrastructure.

References

[1] P. Ripka, *Magnetic sensors and magnetometers, 2nd edition*, Boston, London: Artech House, 2021.

[2] C. Zheng, K. Zhu, S. C. de Freitas *et al.*, "Magnetoresistive Sensor Development Roadmap (Non-Recording Applications)," *Ieee Transactions on Magnetics*, vol. 55, no. 4, Apr, 2019.

[3] T. Reininger, F. Welker, and M. von Zeppelin, "Sensors in position control applications for industrial automation," *Sensors and Actuators a-Physical*, vol. 129, no. 1-2, pp. 270-274, May, 2006.

[4] P. Ripka, J. Blažek, M. Mirzaei *et al.*, "Inductive Position and Speed Sensors," *Sensors*, vol. 20, no. 1, 2019.

[5] S. Tumanski, "Modern magnetic field sensors – a review," *PRZEGLAD ELEKTROTECHNICZNY* vol. 89, no. 10, pp. 12, 2013.

[6] B. George, Z. C. Tan, and S. Nihtianov, "Advances in Capacitive, Eddy Current, and Magnetic Displacement Sensors and Corresponding Interfaces," *Ieee Transactions on Industrial Electronics*, vol. 64, no. 12, pp. 9595-9607, Dec, 2017.

[7] M. Smelko, P. Lipovsky, K. Draganova *et al.*, "Low Frequency Magnetic Fields and Safety," *Acta Physica Polonica A*, vol. 137, no. 5, pp. 693-696, May, 2020.

[8] T. Feng, S. H. Hao, M. H. Hao *et al.*, "Development of a combined magnetic encoder," *Sensor Review*, vol. 36, no. 4, pp. 386-396, 2016.

[9] J. O. Manyala, T. Fritz, and M. Z. Atashbar, "Integration of Triaxial Hall-Effect Sensor Technology for Gear Position Sensing in Commercial Vehicle Transmissions," *Ieee Transactions on Instrumentation and Measurement*, vol. 61, no. 3, pp. 664-672, Mar, 2012.

[10] P. Ribeiro, M. Neto, and S. Cardoso, "Strategy for Determining a Magnet Position in a 2-D Space Using 1-D Sensors," *Ieee Transactions on Magnetics*, vol. 54, no. 11, Nov, 2018.
[11] M. Ortner, M. Ribeiro, and D. Spitzer, "Absolute Long-Range Linear Position System With a Single 3-D Magnetic Field Sensor," *Ieee Transactions on Magnetics*, vol. 55, no. 1, Jan, 2019.
[12] A. Rashid, and O. Hasan, "Wearable technologies for hand joints monitoring for rehabilitation: A survey," *Microelectronics Journal*, vol. 88, pp. 173-183, Jun, 2019.
[13] R. Madson, and R. Rajamani, "Magnetic Position Estimation in Ferromagnetic Systems Involving Significant Hysteresis," *Ieee-Asme Transactions on Mechatronics*, vol. 23, no. 4, pp. 1555-1563, Aug, 2018.
[14] S. Taghvaeeyan, and R. Rajamani, "Magnetic Sensor-Based Large Distance Position Estimation With Disturbance Compensation," *Ieee Sensors Journal*, vol. 15, no. 8, pp. 4249-4258, Aug, 2015.
[15] B. Slusarek, and K. Zakrzewski, "Magnetic properties of permanent magnets for magnetic sensors working in wide range of temperature," *Przeglad Elektrotechniczny*, vol. 88, no. 7B, pp. 123-126, 2012.
[16] S. Taghvaeeyan, R. Rajamani, and Z. X. Sun, "Non-Intrusive Piston Position Measurement System Using Magnetic Field Measurements," *Ieee Sensors Journal*, vol. 13, no. 8, pp. 3106-3114, Aug, 2013.
[17] D. X. Wang, J. Brown, T. Hazelton *et al.*, "360 degrees angle sensor using spin valve materials with SAF structure," *Ieee Transactions on Magnetics*, vol. 41, no. 10, pp. 3700-3702, Oct, 2005.
[18] P. Adamiec, J. Barbero, E. Cordero *et al.*, "Radiation Hard Contactless Angular Position Sensor Based on Hall Effect," *Ieee Transactions on Nuclear Science*, vol. 63, no. 6, pp. 2971-2978, Dec, 2016.
[19] O. Erb, G. Hinz, and N. Preusse, "PLCD, A NOVEL MAGNETIC DISPLACEMENT SENSOR," *Sensors and Actuators a-Physical*, vol. 26, no. 1-3, pp. 277-282, Mar, 1991.
[20] J. Gao, W. F. O. Muller, F. Greiner *et al.*, "Combined Simulation of a Micro Permanent Magnetic Linear Contactless Displacement Sensor," *Sensors*, vol. 10, no. 9, pp. 8424-8436, Sep, 2010.
[21] "https://www.posital.com/en/products/wiegand-sensors/wiegand-sensors.php."
[22] P. Kollu, S. S. Yoon, C. O. Kim *et al.*, "Factors influencing the sensitivity of the CDMPI sensor," *Advances in Nanomaterials and Processing, Pts 1 and 2*, Solid State Phenomena B. T. Ahn, H. Jeon, B. Y. Hur *et al.*, eds., pp. 887-+, Durnten-Zurich: Trans Tech Publications Ltd, 2007.
[23] X. Y. Sun, T. Yamada, and Y. Takemura, "Output Characteristics and Circuit Modeling of Wiegand Sensor," *Sensors*, vol. 19, no. 13, Jul, 2019.
[24] K. Takahashi, T. Yamada, and Y. Takemura, "Circuit Parameters of a Receiver Coil Using a Wiegand Sensor for Wireless Power Transmission," *Sensors*, vol. 19, no. 12, Jun, 2019.
[25] C. C. Chang, J. Y. Chang, and Ieee, "Novel Wiegand Effect-Based Energy Harvesting Device for Linear Positioning Measurement System," *2018 Asia-Pacific Magnetic Recording Conference (Apmrc)*, 2018.
[26] S. N. Nejad, and R. Mansour, "Development of MEMS Reed Magnetic Sensors," *Ieee Transactions on Magnetics*, vol. 52, no. 2, pp. 7, Feb, 2016.
[27] P. Ripka, *Magnetic sensors and magnetometers*, Boston, London: Artech House, 2001.
[28] "POSIC SA https://www.posic.com/EN/inductive-encoder-technology.html."

[29] H. S. Hsiao, and J. Y. Chang, "Characterization of Signal Integrity Due to Pitch-Roll-Yaw Rotation Tolerance in Magnetic Position Sensing Systems," *Ieee Transactions on Magnetics*, vol. 53, no. 3, Mar, 2017.
[30] "KOHDEN Ltd. https://www.hkd.co.jp/english/amr_tec_suichoku/."
[31] S. Paul, J. Chang, A. Rajan *et al.*, "Design of Linear Magnetic Position Sensor Used in Permanent Magnet Linear Machine With Consideration of Manufacturing Tolerances," *Ieee Sensors Journal*, vol. 19, no. 13, pp. 5239-5248, Jul, 2019.
[32] S. W. Du, J. C. Hu, Y. Zhu *et al.*, "An Improved Displacement Measurement Based on Model Reconstruction for Permanent Magnet Synchronous Motor," *Ieee Transactions on Instrumentation and Measurement*, vol. 66, no. 11, pp. 3044-3051, Nov, 2017.
[33] X. Y. Liu, C. H. Liu, and P. W. T. Pong, "Velocity Measurement Technique for Permanent Magnet Synchronous Motors Through External Stray Magnetic Field Sensing," *Ieee Sensors Journal*, vol. 18, no. 10, pp. 4013-4021, May, 2018.
[34] J. Quasdorf, "The Vernier Scale Goes Digital," *Sensors Magazine*, 2009.
[35] Z. J. Zhang, F. L. Ni, Y. Y. Dong *et al.*, "A Novel Absolute Magnetic Rotary Sensor," *Ieee Transactions on Industrial Electronics*, vol. 62, no. 7, pp. 4408-4419, Jul, 2015.
[36] D. B. Denic, and G. S. Miljkovic, "Code reading synchronization method for pseudorandom position encoders," *Sensors and Actuators a-Physical*, vol. 150, no. 2, pp. 188-191, Mar, 2009.
[37] www.rls.si.
[38] S. Fericean, and R. Droxler, "New noncontacting inductive analog proximity and inductive linear displacement sensors for industrial automation," *Ieee Sensors Journal*, vol. 7, no. 11-12, pp. 1538-1545, Nov-Dec, 2007.
[39] S. D. Welsby, and T. Hitz, "True Position Measurement with Eddy Current Technology," *Sensors*, no. 11, pp. 30-40, 1997.
[40] A. Bertacchini, M. Lasagni, and G. Sereni, "Effects of the Target on the Performance of an Ultra-Low Power Eddy Current Displacement Sensor for Industrial Applications," *Electronics*, vol. 9, no. 8, Aug, 2020.
[41] K. D. AnimAppiah, and S. M. Riad, "Analysis and design of ferrite cores for eddy-current-killed oscillator inductive proximity sensors," *Ieee Transactions on Magnetics*, vol. 33, no. 3, pp. 2274-2281, May, 1997.
[42] P. A. Passeraub, P. A. Besse, and R. S. Popovic, "Temperature compensation of an integrated low power inductive proximity microsensor," *Sensors and Actuators a-Physical*, vol. 82, no. 1-3, pp. 62-68, May, 2000.
[43] H. Bartsch, T. Geiling, and J. Muller, "A LTCC low-loss inductive proximity sensor for harsh environments," *Sensors and Actuators a-Physical*, vol. 175, pp. 28-34, Mar, 2012.
[44] P. H. Lo, S. H. Tseng, J. H. Yeh *et al.*, "Development of a proximity sensor with vertically monolithic integrated inductive and capacitive sensing units," *Journal of Micromechanics and Microengineering*, vol. 23, no. 3, Mar, 2013.
[45] A. J. Grobler, G. van Schoor, and E. O. Ranft, "DESIGN AND OPTIMISATION OF A PCB EDDY CURRENT DISPLACEMENT SENSOR," *Saiee Africa Research Journal*, vol. 108, no. 1, pp. 4-11, Mar, 2017.
[46] P. Ripka, J. Vyhnanek, M. Janosek *et al.*, "AMR proximity sensor with inherent demodulation," *IEEE Sensors Journal*, vol. 14, no. 9, pp. 3119-3123, 2014, 2014.
[47] E. Cardelli, A. Faba, and F. Tissi, "Contact-Less Speed Probe Based on Eddy Currents," *Ieee Transactions on Magnetics*, vol. 49, no. 7, pp. 3897-3900, Jul, 2013.
[48] M. Mirzaei, P. Ripka, A. Chirtsov *et al.*, "Eddy Current Linear Speed Sensor," *Ieee Transactions on Magnetics*, vol. 55, no. 1, Jan, 2019.

[49] M. Mirzaei, P. Ripka, A. Chirtsov *et al.*, "Design and modeling of a linear speed sensor with a flat type structure and air coils," *Journal of Magnetism and Magnetic Materials*, vol. 495, Feb, 2020.
[50] S. H. Yang, K. Hirata, T. Ota *et al.*, "Impedance Linearity of Contactless Magnetic-Type Position Sensor," *Ieee Transactions on Magnetics*, vol. 53, no. 6, Jun, 2017.
[51] J. de Pelegrin, B. M. de Carvalho, F. L. Bertotti *et al.*, "Development and Evaluation of a Linear Variable Differential Sensor," *2017 2nd International Symposium on Instrumentation Systems, Circuits and Transducers (Inscit)*, pp. 117-122, 2017.
[52] A. Masi, S. Danzeca, R. Losito *et al.*, "A high precision radiation-tolerant LVDT conditioning module," *Nuclear Instruments & Methods in Physics Research Section a-Accelerators Spectrometers Detectors and Associated Equipment*, vol. 745, pp. 73-81, May, 2014.
[53] V. Gunasekaran, B. George, S. Aniruddhan *et al.*, "Performance Analysis of Oscillator-Based Read-Out Circuit for LVDT," *Ieee Transactions on Instrumentation and Measurement*, vol. 68, no. 4, pp. 1080-1088, Apr, 2019.
[54] H. Ganesan, B. George, S. Aniruddhan *et al.*, "A Dual Slope LVDT-to-Digital Converter," *Ieee Sensors Journal*, vol. 19, no. 3, pp. 868-876, Feb, 2019.
[55] H. Ganesan, B. George, and S. Aniruddhan, "Design and Analysis of a Relaxation Oscillator-Based Interface Circuit for LVDT," *Ieee Transactions on Instrumentation and Measurement*, vol. 68, no. 5, pp. 1261-1270, May, 2019.
[56] K. Banerjee, B. Dam, K. Majumdar *et al.*, "A Novel FPGA-based LVDT Signal Conditioner," *2013 Ieee International Symposium on Industrial Electronics (Isie)*, 2013.
[57] W. Petchmaneelumka, P. Mano, and V. Riewruja, "Linear Variable Differential Transformer Temperature Compensation Technique," *Sensors and Materials*, vol. 30, no. 10, pp. 2171-2181, 2018.
[58] S. K. Mishra, G. Panda, and D. P. Das, "A Novel Method of Extending the Linearity Range of Linear Variable Differential Transformer Using Artificial Neural Network," *Ieee Transactions on Instrumentation and Measurement*, vol. 59, no. 4, pp. 947-953, Apr, 2010.
[59] P. Veeraian, U. Gandhi, and U. Mangalanathan, "Fractional Order Linear Variable Differential Transformer: Design and analysis," *Aeu-International Journal of Electronics and Communications*, vol. 79, pp. 141-150, 2017.
[60] W. Petchmaneelumka, A. Rerkratn, A. Luangpol *et al.*, "Compensation of Temperature Effect for LVDT Transducer," *Journal of Circuits Systems and Computers*, vol. 27, no. 12, Nov, 2018.
[61] W. Petchmaneelumka, W. Koodtalang, and V. Riewruja, "Simple Technique for Linear-Range Extension of Linear Variable Differential Transformer," *Ieee Sensors Journal*, vol. 19, no. 13, pp. 5045-5052, Jul, 2019.
[62] H. Mandal, S. K. Bera, S. Saha *et al.*, "Study of a Modified LVDT Type Displacement Transducer With Unlimited Range," *Ieee Sensors Journal*, vol. 18, no. 23, pp. 9501-9514, Dec, 2018.
[63] H. Sumali, E. P. Bystrom, and G. W. Krutz, "A displacement sensor for nonmetallic hydraulic cylinders," *Ieee Sensors Journal*, vol. 3, no. 6, pp. 818-826, Dec, 2003.
[64] M. Martino, A. Danisi, R. Losito *et al.*, "Design of a Linear Variable Differential Transformer With High Rejection to External Interfering Magnetic Field," *Ieee Transactions on Magnetics*, vol. 46, no. 2, pp. 674-677, Feb, 2010.
[65] A. Grima, M. Di Castro, A. Masi *et al.*, "Electrical Metrological Characterization of Ironless Inductive Position Sensors With Long Cables," *Ieee Sensors Journal*, vol. 18, no. 17, pp. 7114-7121, Sep, 2018.

[66] R. Yanez-Valdez, R. Alva-Gallegos, A. Caballero-Ruiz *et al.*, "Selection of Soft Magnetic Core Materials Used on an LVDT Prototype," *Journal of Applied Research and Technology*, vol. 10, no. 2, pp. 195-205, Apr, 2012.
[67] H. Chiriac, E. Hristoforou, M. Neagu *et al.*, "Linear variable differential transformer sensor using Fe-rich amorphous wires as an active core," *Journal of Applied Physics*, vol. 87, no. 9, pp. 5344-5346, May, 2000.
[68] H. Chiriac, E. Hristoforou, M. Neagu *et al.*, "Linear variable differential transformer sensor using glass-covered amorphous wires as active core," *Journal of Magnetism and Magnetic Materials*, vol. 215, pp. 759-761, Jun, 2000.
[69] P. Ripka, M. Mirzaei, A. Chirtsov *et al.*, "Transformer position sensor for a pneumatic cylinder," *Sensors and Actuators a-Physical*, vol. 294, pp. 91-101, Aug, 2019.
[70] S. M. Djuric, "Performance Analysis of a Planar Displacement Sensor With Inductive Spiral Coils," *Ieee Transactions on Magnetics*, vol. 50, no. 4, Apr, 2014.
[71] N. Anandan, and B. George, "Design and Development of a Planar Linear Variable Differential Transformer for Displacement Sensing," *Ieee Sensors Journal*, vol. 17, no. 16, pp. 5298-5305, Aug, 2017.
[72] M. Podhraski, and J. Trontelj, "A Differential Monolithically Integrated Inductive Linear Displacement Measurement Microsystem," *Sensors*, vol. 16, no. 3, pp. 20, Mar, 2016.
[73] A. Masi, A. Danisi, R. Losito *et al.*, "Characterization of Magnetic Immunity of an Ironless Inductive Position Sensor," *Ieee Sensors Journal*, vol. 13, no. 3, pp. 8, Mar, 2013.
[74] M. Mirzaei, P. Ripka, A. Chirtsov *et al.*, "Temperature stability of the transformer position transducer for pneumatic cylinder," *Journal of Magnetism and Magnetic Materials*, vol. 503, Jun, 2020.
[75] "http://www.inductosyn.com/products.htm."
[76] N. Misron, L. Q. Ying, R. N. Firdaus *et al.*, "Effect of Inductive Coil Shape on Sensing Performance of Linear Displacement Sensor Using Thin Inductive Coil and Pattern Guide," *Sensors*, vol. 11, no. 11, pp. 10522-10533, Nov, 2011.
[77] A. Babu, and B. George, "Design and Development of a New Non-Contact Inductive Displacement Sensor," *Ieee Sensors Journal*, vol. 18, no. 3, pp. 976-984, Feb, 2018.
[78] J. Figueiredo, "Resolver Models for Manufacturing," *Ieee Transactions on Industrial Electronics*, vol. 58, no. 8, pp. 3693-3700, Aug, 2011.
[79] M. Caruso, A. O. Di Tommaso, F. Genduso *et al.*, "A DSP-Based Resolver-To-Digital Converter for High-Performance Electrical Drive Applications," *Ieee Transactions on Industrial Electronics*, vol. 63, no. 7, pp. 4042-4051, Jul, 2016.
[80] V. Sabatini, M. Di Benedetto, and A. Lidozzi, "Synchronous Adaptive Resolver-to-Digital Converter for FPGA-Based High-Performance Control Loops," *Ieee Transactions on Instrumentation and Measurement*, vol. 68, no. 10, pp. 3972-3982, Oct, 2019.
[81] F. A. Karabeyli, and A. Z. Alkar, "Enhancing the Accuracy for the Open-loop Resolver to Digital Converters," *Journal of Electrical Engineering & Technology*, vol. 13, no. 1, pp. 192-200, Jan, 2018.
[82] Z. Nasiri-Gheidari, "Design, Analysis, and Prototyping of a New Wound-Rotor Axial Flux Brushless Resolver," *Ieee Transactions on Energy Conversion*, vol. 32, no. 1, pp. 276-283, Mar, 2017.
[83] H. Saneie, R. Alipour-Sarabi, Z. Nasiri-Gheidari *et al.*, "Challenges of Finite Element Analysis of Resolvers," *Ieee Transactions on Energy Conversion*, vol. 34, no. 2, pp. 973-983, Jun, 2019.

[84] M. B. Coskun, K. Thotahewa, Y. S. Ying *et al.*, "Nanoscale displacement sensing using microfabricated variable-inductance planar coils," *Applied Physics Letters*, vol. 103, no. 14, Sep, 2013.
[85] K. R. Sandra, B. Georg, and V. J. Kumar, "Combined Variable Reluctance-Hall Effect Displacement Sensor," *Ieee Transactions on Instrumentation and Measurement*, vol. 67, no. 5, pp. 1169-1177, May, 2018.
[86] F. Seco, J. M. Martin, and A. R. Jimenez, "Improving the Accuracy of Magnetostrictive Linear Position Sensors," *Ieee Transactions on Instrumentation and Measurement*, vol. 58, no. 3, pp. 722-729, Mar, 2009.
[87] C. Deng, Y. H. Kang, B. Ye *et al.*, "Enhancing MPS Signal by Bipolar Pulse Excitation and Interference of Reflection Wave," *Ieee Transactions on Instrumentation and Measurement*, vol. 63, no. 10, pp. 2464-2471, Oct, 2014.
[88] E. Hristoforou, "Magnetostrictive delay lines: engineering theory and sensing applications," *Measurement Science and Technology*, vol. 14, no. 2, pp. R15-R47, Feb, 2003.
[89] E. Hristoforou, P. D. Dimitropoulos, and J. Petrou, "A new position sensor based on the MDL technique," *Sensors and Actuators a-Physical*, vol. 132, no. 1, pp. 112-121, Nov, 2006.
[90] P. Kemidis, C. Orfanidou, and E. Hristoforou, "Position sensors based on the delay line principle," *Journal of Optoelectronics and Advanced Materials*, vol. 4, no. 2, pp. 347-352, Jun, 2002.
[91] T. Konig, T. Greiner, A. Zern *et al.*, "Using Eddy Currents Within Magnetostrictive Position Sensors for Velocity Estimation," *Ieee Sensors Journal*, vol. 19, no. 15, pp. 6325-6334, Aug, 2019.
[92] J. Jankowski, and C. Sucksdorff, *IAGA Guide for Magnetic Measurements and Observatory Practice*: Available at http://www.iaga-aiga.org/publications/guides/, 1996.
[93] P. Ripka, and A. Zikmund, "Testing and calibration of magnetic sensors," *Sensor Letters*, vol. 11, no. 1, pp. 44-49, 2013, 2013.
[94] J. Včelák, P. Ripka, J. Kubík *et al.*, "AMR navigation systems and methods of their calibration," *Sensors and Actuators, A: Physical*, vol. 123-124, pp. 122-128, 2005, 2005.
[95] M. P. Lassahn, and G. Trenkler, "VECTORIAL CALIBRATION OF 3D MAGNETIC-FIELD SENSOR ARRAYS," *Ieee Transactions on Instrumentation and Measurement*, vol. 44, no. 2, pp. 360-362, Apr, 1995.
[96] D. H. Pan, J. Li, C. Y. Jin *et al.*, "A New Calibration Method for Triaxial Fluxgate Magnetometer Based on Magnetic Shielding Room," *Ieee Transactions on Industrial Electronics*, vol. 67, no. 5, pp. 4183-4192, May, 2020.
[97] J. M. G. Merayo, P. Brauer, F. Primdahl *et al.*, "Scalar calibration of vector magnetometers," *Measurement Science and Technology*, vol. 11, no. 2, pp. 120-132, Feb, 2000.
[98] V. Petrucha, P. Kaspar, P. Ripka *et al.*, "Automated system for the calibration of magnetometers," *Journal of Applied Physics*, vol. 105, no. 7, Apr, 2009.
[99] H. U. Auster, K. H. Fornacon, E. Georgescu *et al.*, "Calibration of flux-gate magnetometers using relative motion," *Measurement Science and Technology*, vol. 13, no. 7, pp. 1124-1131, Jul, 2002.
[100] T. Risbo, P. Brauer, J. M. G. Merayo *et al.*, "Orsted pre-flight magnetometer calibration mission," *Measurement Science and Technology*, vol. 14, no. 5, pp. 674-688, May, 2003.

[101] H. S. Ousaloo, G. Sharifi, J. Mahdian *et al.*, "Complete Calibration of Three-Axis Strapdown Magnetometer in Mounting Frame," *Ieee Sensors Journal,* vol. 17, no. 23, pp. 7886-7893, Dec, 2017.
[102] J. F. Vasconcelos, G. Elkaim, C. Silvestre *et al.*, "Geometric Approach to Strapdown Magnetometer Calibration in Sensor Frame," *Ieee Transactions on Aerospace and Electronic Systems,* vol. 47, no. 2, pp. 1293-1306, Apr, 2011.
[103] R. Costanzi, F. Fanelli, N. Monni *et al.*, "An Attitude Estimation Algorithm for Mobile Robots Under Unknown Magnetic Disturbances," *Ieee-Asme Transactions on Mechatronics,* vol. 21, no. 4, pp. 1900-1911, Aug, 2016.
[104] I. Ashraf, S. Hur, and Y. Park, "BLocate: A Building Identification Scheme in GPS Denied Environments Using Smartphone Sensors," *Sensors,* vol. 18, no. 11, Nov, 2018.
[105] P. Davidson, and R. Piche, "A Survey of Selected Indoor Positioning Methods for Smartphones," *Ieee Communications Surveys and Tutorials,* vol. 19, no. 2, pp. 1347-1370, 2017.
[106] G. X. Liu, L. F. Shi, J. H. Xun *et al.*, "An orientation estimation algorithm based on multi-source information fusion," *Measurement Science and Technology,* vol. 29, no. 11, Nov, 2018.
[107] S. Qiu, Z. L. Wang, H. Y. Zhao *et al.*, "Inertial/magnetic sensors based pedestrian dead reckoning by means of multi-sensor fusion," *Information Fusion,* vol. 39, pp. 108-119, Jan, 2018.
[108] M. N. Muhammad, Z. Salcic, and K. I. K. Wang, "Indoor Pedestrian Tracking Using Consumer-Grade Inertial Sensors With PZTD Heading Correction," *Ieee Sensors Journal,* vol. 18, no. 12, pp. 5164-5172, Jun, 2018.
[109] H. S. Kim, W. Seo, and K. R. Baek, "Indoor Positioning System Using Magnetic Field Map Navigation and an Encoder System," *Sensors,* vol. 17, no. 3, Mar, 2017.
[110] B. Gozick, K. P. Subbu, R. Dantu *et al.*, "Magnetic Maps for Indoor Navigation," *Ieee Transactions on Instrumentation and Measurement,* vol. 60, no. 12, pp. 3883-3891, Dec, 2011.
[111] M. Abayazid, T. Kato, S. Silverman *et al.*, "Using needle orientation sensing as surrogate signal for respiratory motion estimation in percutaneous interventions," *International Journal of Computer Assisted Radiology and Surgery,* vol. 13, no. 1, pp. 125-133, Jan, 2018.
[112] M. Hehn, E. Sippel, C. Carlowitz *et al.*, "High-Accuracy Localization and Calibration for 5-DoF Indoor Magnetic Positioning Systems," *Ieee Transactions on Instrumentation and Measurement,* vol. 68, no. 10, pp. 4135-4145, Oct, 2019.
[113] P. Lipovsky, K. Draganova, M. Smelko *et al.*, "Vector Magnetometer used as Magnetometric Security Subsystem," *International Conference on Military Technologies*. pp. 527-530, 2015.
[114] F. Attivissimo, A. M. L. Lanzolla, S. Carlone *et al.*, "A novel electromagnetic tracking system for surgery navigation," *Computer Assisted Surgery,* vol. 23, no. 1, pp. 42-52, 2018.
[115] M. Sha, Y. F. Wang, N. Ding *et al.*, "An electromagnetic tracking method based on fast determination of the maximum magnetic flux density vector represented by two azimuth angles," *Measurement,* vol. 109, pp. 160-167, Oct, 2017.
[116] G. L. Shao, Y. C. Tang, L. Q. Tang *et al.*, "A Novel Passive Magnetic Localization Wearable System for Wireless Capsule Endoscopy," *Ieee Sensors Journal,* vol. 19, no. 9, pp. 3462-3472, May, 2019.

[117] C. Hu, Y. P. Ren, X. H. You *et al.*, "Locating Intra-Body Capsule Object by Three-Magnet Sensing System," *Ieee Sensors Journal,* vol. 16, no. 13, pp. 5167-5176, Jul, 2016.
[118] K. O'Donoghue, D. Eustace, J. Griffiths *et al.*, "Catheter Position Tracking System Using Planar Magnetics and Closed Loop Current Control," *Ieee Transactions on Magnetics,* vol. 50, no. 7, Jul, 2014.
[119] C. R. Taylor, H. G. Abramson, and H. M. Herr, "Low-Latency Tracking of Multiple Permanent Magnets," *Ieee Sensors Journal,* vol. 19, no. 23, pp. 11458-11468, Dec, 2019.
[120] D. Cichon, R. Psiuk, H. Brauer *et al.*, "A Hall-Sensor-Based Localization Method With Six Degrees of Freedom Using Unscented Kalman Filter," *Ieee Sensors Journal,* vol. 19, no. 7, pp. 2509-2516, Apr, 2019.
[121] I. S. M. Khalil, A. Adel, D. Mahdy *et al.*, "Magnetic localization and control of helical robots for clearing superficial blood clots," *Apl Bioengineering,* vol. 3, no. 2, Jun, 2019.
[122] S. Daroogheha, T. A. Lasky, and B. Ravani, "Position Measurement Under Uncertainty Using Magnetic Field Sensing," *Ieee Transactions on Magnetics,* vol. 54, no. 12, Dec, 2018.
[123] C. Y. Chan, "Magnetic sensing as a position reference system for ground vehicle control," *Ieee Transactions on Instrumentation and Measurement,* vol. 51, no. 1, pp. 43-52, Feb, 2002.
[124] S. Hashi, M. Toyoda, S. Yabukami *et al.*, "Wireless magnetic motion capture system using multiple LC resonant magnetic markers with high accuracy," *Sensors and Actuators a-Physical,* vol. 142, no. 2, pp. 520-527, Apr, 2008.
[125] S. Hashi, S. Yabukami, H. Kanetaka *et al.*, "Numerical Study on the Improvement of Detection Accuracy for a Wireless Motion Capture System," *Ieee Transactions on Magnetics,* vol. 45, no. 6, pp. 2736-2739, Jun, 2009.
[126] F. H. Raab, E. B. Blood, T. O. Steiner *et al.*, "MAGNETIC POSITION AND ORIENTATION TRACKING SYSTEM," *Ieee Transactions on Aerospace and Electronic Systems,* vol. 15, no. 5, pp. 709-718, 1979.
[127] C. Hu, S. Song, X. J. Wang *et al.*, "A Novel Positioning and Orientation System Based on Three-Axis Magnetic Coils," *Ieee Transactions on Magnetics,* vol. 48, no. 7, pp. 2211-2219, Jul, 2012.
[128] W. Kim, J. Song, and F. C. Park, "Closed-Form Position and Orientation Estimation for a Three-Axis Electromagnetic Tracking System," *Ieee Transactions on Industrial Electronics,* vol. 65, no. 5, pp. 4331-4337, May, 2018.
[129] "https://www.ndigital.com/."
[130] H. D. Dai, S. Song, X. P. Zeng *et al.*, "6-D Electromagnetic Tracking Approach Using Uniaxial Transmitting Coil and Tri-Axial Magneto-Resistive Sensor," *Ieee Sensors Journal,* vol. 18, no. 3, pp. 1178-1186, Feb, 2018.
[131] M. Lapinski, C. B. Medeiros, D. M. Scarborough *et al.*, "A Wide-Range, Wireless Wearable Inertial Motion Sensing System for Capturing Fast Athletic Biomechanics in Overhead Pitching," *Sensors,* vol. 19, no. 17, Sep, 2019.
[132] A. T. Maereg, E. L. Secco, T. F. Agidew *et al.*, "A Low-Cost, Wearable Opto-Inertial 6-DOF Hand Pose Tracking System for VR," *Technologies,* vol. 5, no. 3, Sep, 2017.
[133] A. M. Franz, T. Haidegger, W. Birkfellner *et al.*, "Electromagnetic Tracking in Medicine-A Review of Technology, Validation, and Applications," *Ieee Transactions on Medical Imaging,* vol. 33, no. 8, pp. 1702-1725, Aug, 2014.
[134] Z. H. Wang, M. Poscente, D. Filip *et al.*, "Rotary in-drilling alignment using an autonomous MEMS-based inertial measurement unit for measurement- while-drilling

processes," *Ieee Instrumentation & Measurement Magazine*, vol. 16, no. 6, pp. 26-34, Dec, 2013.
[135] J. Vcelak, P. Ripka, and A. Zikmund, "Long-Range Magnetic Tracking System," *Ieee Sensors Journal*, vol. 15, no. 1, pp. 491-496, Jan, 2015.
[136] T. Liu, and B. X. Wang, "Study of magnetic ranging technology in horizontal directional drilling," *Sensors and Actuators a-Physical*, vol. 171, no. 2, pp. 186-190, Nov, 2011.
[137] Z. W. Liu, and J. C. Song, "A Low-Cost Calibration Strategy for Measurement-While-Drilling System," *Ieee Transactions on Industrial Electronics*, vol. 65, no. 4, pp. 3559-3567, Apr, 2018.
[138] L. N. S. Alconcel, P. Fox, P. Brown *et al.*, "An initial investigation of the long-term trends in the fluxgate magnetometer (FGM) calibration parameters on the four Cluster spacecraft," *Geoscientific Instrumentation Methods and Data Systems*, vol. 3, no. 2, pp. 95-109, 2014.
[139] P. Alken, N. Olsen, and C. C. Finlay, "Co-estimation of geomagnetic field and in-orbit fluxgate magnetometer calibration parameters," *Earth Planets and Space*, vol. 72, no. 1, Apr, 2020.
[140] B. Park, and H. Myung, "Resilient Underground Localization Using Magnetic Field Anomalies for Drilling Environment," *Ieee Transactions on Industrial Electronics*, vol. 65, no. 2, pp. 1377-1387, Feb, 2018.
[141] L. G. S. Fortaleza, E. C. Monteiro, C. R. H. Barbosa *et al.*, "Biomedical comparison of magnetometers for non-ferromagnetic metallic foreign body detection," *Journal of Physics Conference Series*, 2018.
[142] P. Lipovsky, K. Draganova, J. Novotnak *et al.*, "Indoor Mapping of Magnetic Fields Using UAV Equipped with Fluxgate Magnetometer," *Sensors*, vol. 21, no. 12, Jun, 2021.
[143] A. Danisi, A. Masi, R. Losito *et al.*, "Modeling of High-Frequency Electromagnetic Effects on an Ironless Inductive Position Sensor," *Ieee Sensors Journal*, vol. 13, no. 12, pp. 4663-4670, Dec, 2013.
[144] A. Danisi, A. Masi, and R. Losito, "Performance Analysis of the Ironless Inductive Position Sensor in the Large Hadron Collider Collimators Environment," *Sensors*, vol. 15, no. 11, pp. 28592-28602, Nov, 2015.
[145] G. T. Laskoski, S. F. Pichorim, and P. J. Abatti, "Distance Measurement With Inductive Coils," *Ieee Sensors Journal*, vol. 12, no. 6, pp. 2237-2242, Jun, 2012.
[146] J. Tomek, P. Mlejnek, V. Janásek *et al.*, "The precision of gastric motility and volume sensing by implanted magnetic sensors," *Sensors and Actuators, A: Physical*, vol. 142, no. 1, pp. 34-39, 2008, 2008.
[147] T. Liu, and B. X. Wang, "Guidance Method in HDD Based on Rotating Magnetic Field," *Ieee Transactions on Geoscience and Remote Sensing*, vol. 52, no. 1, pp. 71-75, Jan, 2014.
[148] A. Zikmund, and P. Ripka, "A magnetic distance sensor with high precision," *Sensors and Actuators, A: Physical*, vol. 186, pp. 137-142, 2012, 2012.
[149] J. Blazek, D. Praslicka, J. Hudak *et al.*, "New Generation of Magnetic Relaxation Sensors Based on the Melt-Spun FeCoBCu Alloys," *Acta Physica Polonica A*, vol. 118, no. 5, pp. 1010-1012, Nov, 2010.
[150] D. Praslicka, J. Blazek, J. Hudak *et al.*, "INDUSTRIAL APPLICATIONS OF MAGNETOMETRY," *Journal of Electrical Engineering-Elektrotechnicky Casopis*, vol. 66, no. 7, pp. 190-192, Dec, 2015.
[151] P. Ripka, J. Včelák, P. Kašpar *et al.*, "Bomb detection in magnetic soils: AC versus DC methods." pp. 1389-1391.

[152] P. Ripka, "Contactless measurement of electric current using magnetic sensors," *Technisches Messen,* vol. Early access 10.1515/teme-2019-0032, 2019
[153] Y. B. Gao, C. Duan, A. A. Oliveira *et al.*, "3-D Coil Positioning Based on Magnetic Sensing for Wireless EV Charging," *Ieee Transactions on Transportation Electrification,* vol. 3, no. 3, pp. 578-588, Sep, 2017.
[154] S. Y. Jeong, H. G. Kwak, G. C. Jang *et al.*, "Dual-Purpose Nonoverlapping Coil Sets as Metal Object and Vehicle Position Detections for Wireless Stationary EV Chargers," *Ieee Transactions on Power Electronics,* vol. 33, no. 9, pp. 7387-7397, Sep, 2018.
[155] W. Han, K. T. Chau, C. Q. Jiang *et al.*, "Accurate Position Detection in Wireless Power Transfer Using Magnetoresistive Sensors for Implant Applications," *Ieee Transactions on Magnetics,* vol. 54, no. 11, Nov, 2018.
[156] X. Y. Liu, C. H. Liu, W. Han *et al.*, "Design and Implementation of a Multi-Purpose TMR Sensor Matrix for Wireless Electric Vehicle Charging," *Ieee Sensors Journal,* vol. 19, no. 5, pp. 1683-1692, Mar, 2019.
[157] S. Tumanski, "Induction coil sensors - a review," *Measurement Science and Technology,* vol. 18, no. 3, pp. R31-R46, Mar, 2007.
[158] P. Arpaia, B. Celano, L. De Vito *et al.*, "Measuring the magnetic axis alignment during solenoids working," *Scientific Reports,* vol. 8, Jul, 2018.